Chapter 1 - INTRODUCTION

1.1 Background

Disorders of the wrist are a common clinical problem in our community (Grieco et al., 1998; Larsen and Lauritsen, 1993; Morgan and Linder, 1997; Nordstrom et al., 1998; Prince et al., 1993). The consequences of wrist disorders can be debilitating, as the wrist may be unable to stabilise the hand to perform activities of daily living (Bogumill, 1977; Kapandji, 1982; Norkin and Levangie, 1984; Weber, 1997). These disabilities lead to a reduction in productivity and require the use of considerable community resources (Dorsay et al., 2001; Kelsey et al., 1997).

Despite the importance of the wrist to function, the development of knowledge of the wrist and its disorders has been slow. At times the wrist has been ignored. As seen in the medieval drawing of the hand and forearm which completely omits the wrist (Figure 1.1).

Figure 1.1 - Drawing from a medieval text shows omission of the carpus.

One reason for the delay in development of understanding of the wrist is related to its complexity. It is a perplexing area of musculoskeletal anatomy. There are eight small bones divided into 2 rows and 3 columns (Craigen and Stanley, 1995; Navarro, 1921; Taleisnik, 1976). These bones are connected by a mesh of ligaments that allow transmission of force with dexterity in six directions. All in less than 5cm!

Despite the slow initial development there have been exponential advances in the understanding of the normal and abnormal wrist in the areas of anatomy, imaging and surgery particularly in the last 20 years. Advances in one area often provide the basis for development in another area.

1.1.1 Anatomy

There has been a progressive advance of the understanding of wrist anatomy. These developments include an understanding of the wrist morphology (Kauer, 1986; Viegas, 1990; Viegas et al., 1993; Weber, 1984), kinematics (Craigen and Stanley, 1995; Garcia-Elias et al., 1995; Landsmeer, 1961; Lichtman et al., 1981; Moritomo et al., 2006; Morrey and An, 1985; Navarro, 1921; Taleisnik, 1976; von Bonin, 1929) and carpal instability (Linscheid et al., 1972; Mayfield et al., 1980). This knowledge interfaces with imaging and surgery for the wrist. Viegas described two different types of lunate morphology (Viegas et al., 1993) Craigen and Stanley described a spectrum of kinematics of the normal scaphoid (Craigen and Stanley, 1995). However there has not been a description of the association between the lunate morphology and scaphoid kinematics ranging from row to column.

1.1.2 Imaging

In 1895 Roentgen developed the technique of radiology using x-rays. The first radiological image was of his wife's hand (Figure 1.2) with the characteristic omission of the wrist! Over the next one hundred years plain radiography has been the mainstay of imaging of the wrist, although interpretation has been challenging (Biondetti et al., 1987; Engdahl and Schacherer, 1989; Friedman et al., 1990). Advances in the methods, techniques and interpretation of radiological imaging of the wrist have been considerable. These include different methods of performing the radiographs and development of specialised views to demonstrate the carpus (Berna et al., 1998; Berna et al., 1993; Gaebler et al., 1998; Proubasta et al., 1989). Arthrography of the wrist has been utilised to assess carpal instability (Brown et al., 1994). Bone scans have been used to identify if an occult scaphoid fracture is present (Tiel-van Buul et al., 1993; Tiel-van Buul et al., 1993). Trispiral tomography has been utilised to assess deformity of the scaphoid (Amadio et al., 1989). Fluoroscopy has been used in the kinematic assessment of carpal instability (Braunstein et al., 1985; Protas and Jackson, 1980; White et al., 1984). More recently, assessment of the carpus has been performed with more advanced

technologies, including computed tomography (CT) scanning (Friedman et al., 1990; Sanders, 1988) and magnetic resonance imaging (MRI) (Cerofolini et al., 1990; Sullivan and Berquist, 1991).

Despite these advances there remains difficulty assessing scaphoid fractures.

Figure 1.2 - First radiological image created by Roentgen in 1895. It shows the osteology of the hand, but omits to include the wrist. Public domain image from National Library of Medicine.

1.1.3 Arthroscopy

The advances in wrist surgery have been substantial. The initial surgical options were salvage in nature and included amputation, total wrist fusion and distal ulnar resection. These procedures have been effective in providing pain relief, although with a considerable morbidity (Darrah, 1912; Dingman, 1952; Field et al., 1996; Papaioannou and Dickson, 1982; Stanley et al., 1986).

Open surgical reconstructive procedures have developed as a consequence of a greater understanding of the functional anatomy (Watson et al., 1986). These procedures were developed to maintain motion while still providing pain relief. These include scaphotrapezotrapezoidal (STT) joint arthrodesis, proximal row carpectomy and hemi-resection of the distal ulna (Bowers, 1985; Ferlic et al., 1991; Watson and Eaton, 1987; Watson, 1980; Watson et al., 1986). Open procedures have been the mainstay of surgical management of disorders of the wrist, but have been associated with a slow rehabilitation and post-operative stiffness (Figure 1.3) (Field et al., 1996; Tham and Ireland, 1992).

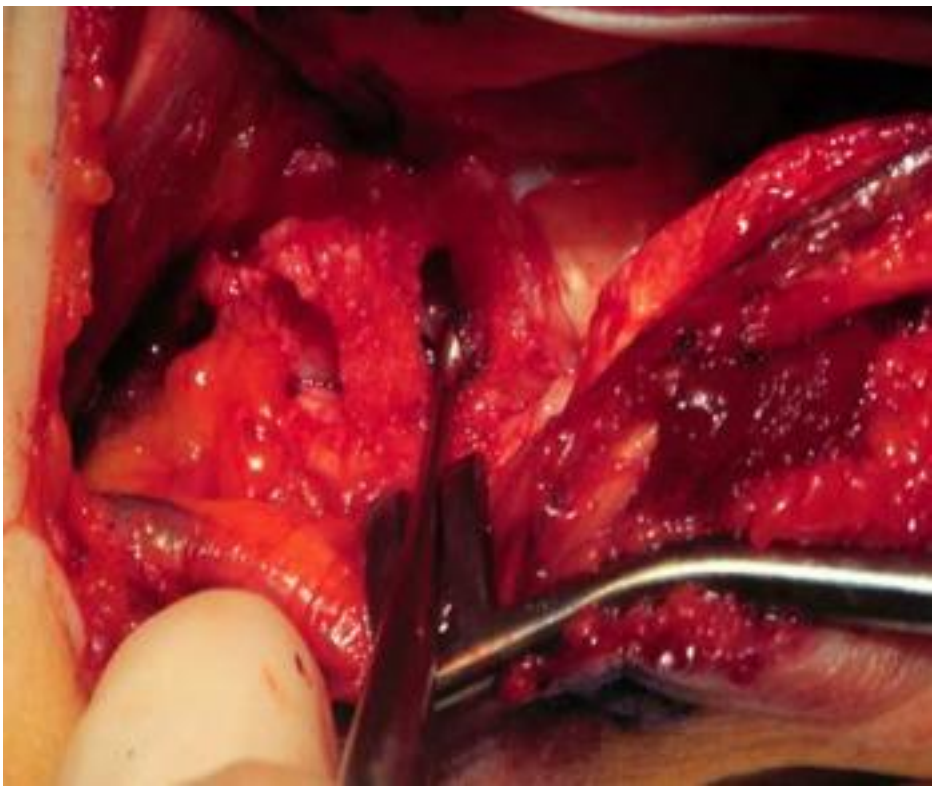

Figure 1.3 – An open volar approach to a large intra-osseous ganglion of the lunate. With this exposure through the floor of the carpal tunnel the patient developed a contracture of the wrist. This complication raises the question, how to treat this complication and how to prevent it. Image from private file.

Professor Kenji Ta-kagi performed the first arthroscopy in 1920. Owing to the need to have miniaturisation of equipment, it was not until 1979 that wrist arthroscopy was first performed by Chen (Chen, 1979). By this time arthroscopy of the knee was popular and had gone from a

simple diagnostic procedure to a therapeutic modality. In 1986 the first instructional course lecture on wrist arthroscopy was presented at the American Academy of Orthopaedic Surgeons meeting (Roth et al., 1988). This made wrist arthroscopy a topical subject and brought this procedure to the community orthopaedic surgeon. Wrist arthroscopy became an important diagnostic tool and was subsequently reported to be superior to fluoroscopy for the assessment of reduction of distal radius fractures and arthrography in the assessment of the carpal instability and Trainaglar Fibro-Cartilage (TFC) tears (Cooney and Berger, 1993; Edwards et al., 2001; Roth and Haddad, 1986).

The development of small joint instrumentation enabled therapeutic arthroscopy to develop (Roth et al., 1988; Whipple, 1988). Therapeutic arthroscopy commenced with “ectomy” procedures (Oni, 1997; Roth and Poehling, 1990) and has extended to more advanced techniques, such as arthroscopic assisted fixation of wrist fractures (Culp and Osterman, 1995; Whipple, 1995; Whipple, 1995).

Despite these significant advances in wrist arthroscopy, it is overshadowed by the advanced understanding of anatomy and development of techniques that have been reported in the knee and shoulder (Arnoczky and Warren, 1982; Hefzy and Grood, 1988; McIntyre and Caspari, 1993; Muller, 1983; Warren and Marshall, 1979). Advanced reconstructive surgery on the knee and shoulder have led to improved patient outcomes and enabled patients to return to work, sport and activities of daily living.

There remains considerable opportunity to further develop the knowledge of anatomy, imaging and arthroscopy and to transfer this into the clinical and surgical practice in a safe and efficient manner.

1.2 Aims of thesis.

1. To develop the understanding of the normal and abnormal wrist, specifically in the areas of anatomy, imaging and arthroscopy.

2. To advance the understanding of morphology and kinematics of the normal wrist.

3. To advance the understanding of imaging of the abnormal wrist.

4. To advance the practice of wrist arthroscopy.

1.3 Significance of aims.

An understanding of wrist anatomy is built on the development of knowledge of the normal wrist morphology (shape) and kinematics (movement). To develop the understanding of the morphology of the each component of the wrist is important. With this understanding a better appreciation of the kinematic and function of the wrist can be obtained. Having built these fundamental anatomical principles, the clinician can apply them when assessing the clinical and radiological aspects of the abnormal wrist. This is of value to the clinician who attempts to obtain a diagnosis before embarking upon treatment.

The surgeon requires good anatomical knowledge of the normal wrist and the clinical and radiological assessment of the abnormal wrist when considering the surgical treatment. The surgeon's role is to change the abnormal anatomy, with the aim of improving the patient's symptoms. Therefore the basic understanding of normal human anatomy and the understanding of the abnormal anatomy in the individual patient are critical to the outcome of the patient. With the use of anatomically directed modern imaging modalities, more detailed clinically relevant information can be obtained to enable an anatomically specific diagnosis to be made.

Armed with an anatomic specific diagnosis, the surgeon is better prepared to consider the treatment options of the clinical disorder, and is not required to resort to the salvage surgical options. Using the technical advances in arthroscopy, the surgeon can now add to the list of surgical treatment options, diagnostic and therapeutic wrist arthroscopy.

The development of new techniques in wrist arthroscopy is likely to provide a wider array of surgical options to the surgeon which is more specific to the anatomical problem of the individual patient. The surgeon will not have to rely on the salvage surgical option to treat the

patient's pain. These new options include advanced arthroscopic procedures that have less morbidity and lower complication rates. As the morbidity reduces, the surgical options can be applied to a wider spectrum of wrist disorders and not just to the patient with a severe disability. Therefore, the overall significance of the aims of this thesis, is to increase the patients' quality of life and allow them to return to their chosen work, sport and activities of daily living.

1.4 Objectives of thesis

1. To develop an understanding of morphological and kinematic anatomy of the normal wrist, including
    a. kinematics of the scaphoid
    b. morphology of the triquetro-hamate joint
2. To develop clinically relevant imaging of the wrist, including
    a. development of a standardised technique of computed tomography (CT) scanning of the scaphoid
    b. develop methods for assessment of scaphoid deformity
    c. assess the clinical application of CT scanning for scaphoid fractures including pre-operative planning of correction of scaphoid deformity
    d. assess the role of operative fluoroscopy for management of disorders of the wrist and upper limb
3. To develop improved arthroscopic techniques, including in patients with
    a. Kienböck disease
    b. distal radius fracture
    c. STT joint arthritis
    d. intra-osseous ganglion of the lunate
    e. capsular contracture of the wrist
    f. ulnar stylo-carpal impaction

Chapter 2 - LITERATURE REVIEW

2.1 Anatomy

2.1.1 Introduction

The first group of papers deals with anatomy of the wrist, specifically morphology of the mid-carpal joint and kinematics of the scaphoid. The rationale for the studies was that there were important gaps in knowledge in these areas; such as

1) the association between the lunate morphology and the scaphoid kinematics and
2) variation in the described morphology of the triquetro-hamate joint.

Therefore the studies performed in the thesis sought to address these deficiencies.
The literature reviewed specifically deals with scaphoid kinematics and morphology of the mid-carpal joint.

2.1.2 Scaphoid kinematics

Understanding of the fundamentals of carpal anatomy is integral to understanding of carpal morphology and kinematics (Weber, 1984). It is important to consider the different anatomic variations to understand how they can influence carpal kinematics.

Classical anatomists divided the carpus into two rows: a distal row consisting of the hamate, capitate, trapezium and trapezoid; and a proximal row consisting of the triquetrum and lunate, with the scaphoid bridging the two rows. The theory stated that flexion and extension occurred at the mid-carpal joint and radial and ulnar inclination by the scaphoid sliding down the slope of the distal radius (Johnson, 1907). Navaro originally proposed the column theory (Navarro, 1921) in which the carpus is made up of three columns: the central, the lateral and the medial columns. The central column consists of the lunate, capitate and hamate; the lateral column the scaphoid, trapezium and trapezoid; and the medial column the triquetrum and pisiform. Based on an anatomical investigation of the wrist ligaments, Taleisnik modified this theory (Taleisnik, 1976). He believed that the distal row effectively acted as a single unit with the lunate, that the lateral column was formed solely by the scaphoid and the medial column by the triquetrum only. Both researchers believed that the central column controls wrist flexion and extension, with radial and ulnar inclination occurring by rotation of the scaphoid and triquetrum about the central axis.

Viegas reported on the importance of osseous morphology (Viegas et al., 1993). This included the shape of the lunate. The type 1 lunate has a single distal facet for the capitate and does not articulate with the hamate (Figure 2.1). In contrast, a type 2 lunate has two distal facets: the radial-sided facet articulates with the capitate and the ulnar-sided facet articulates with the hamate (Viegas et al., 1993) (Figure 2.2, Figure 2.3). The reported incidence of the type 1 ranges from 27% to 35% and type 2 from 66% to 73% (Burgess, 1990; Kaempffe and Lerner, 1996; Viegas, 1990; Viegas et al., 1993; Viegas et al., 1993). The type of lunate can usually be determined based on plain radiographs, although a small facet may be difficult to identify (Sagerman et al., 1995). Viegas also reported the condyle of the hamate commonly had degenerative arthritis in cadaveric specimens with a type 2 lunate (Viegas et al., 1993).

Figure 2.1 – Type 1 lunate. Wrist radiograph of a type 1 lunate, note the single distal articular facet of the lunate.

Figure 2.2 – Type 2 lunate. Wrist radiograph of a type 2 lunate, note the double distal articular facet of the lunate.

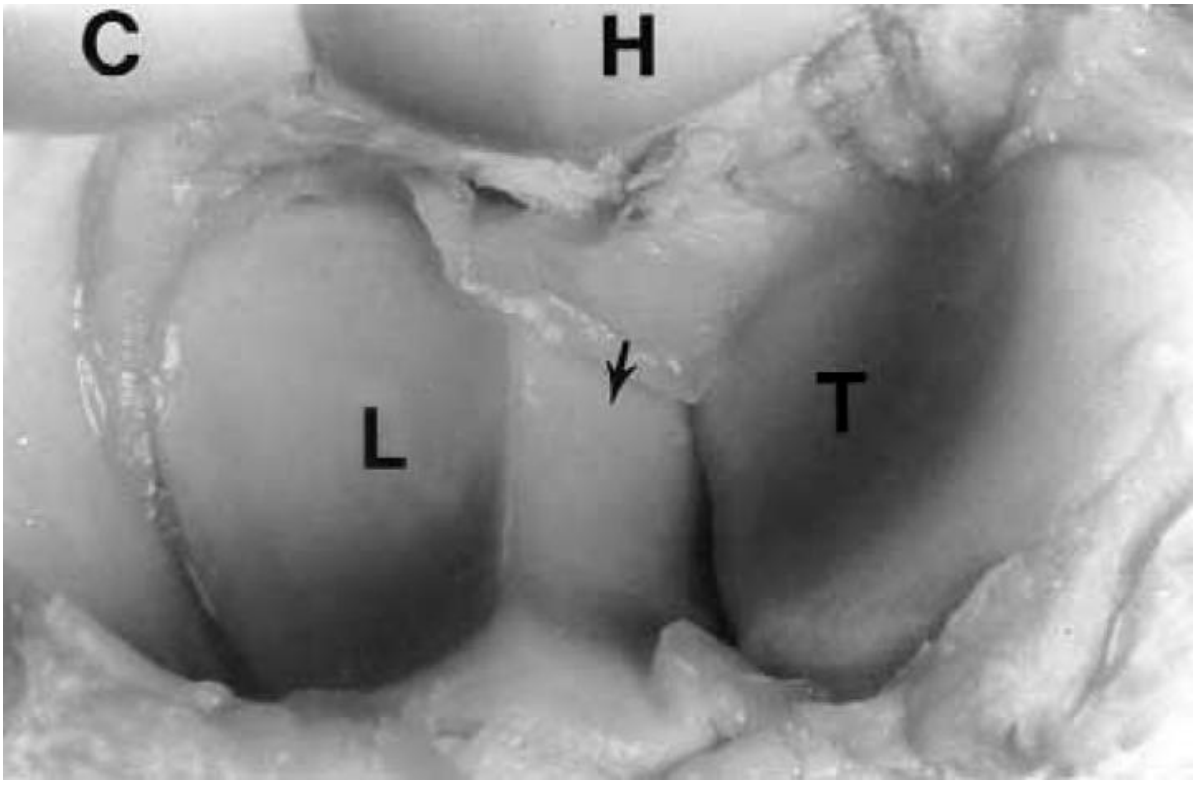

Figure 2.3 – Cadaveric right wrist. Mid-carpal joint with type 2 lunate. Note the large radial sided facet of the lunate (L) and small ulnar sided facet of the lunate (arrow). The hamate (H) articulates with the ulnar facet of the lunate and the triquetrum (T). The capitate (C) articulates with the scaphoid and the radial facet of the lunate. From – Viegas et al., 1990.

Viegas also made a number of observations regarding the curvature of the articular surface of the capitate. A type 1 lunate is associated with a large circle of radius of the proximal aspect of the capitate (Figure 2.4). A type 2 lunate is associated with a small circle of radius of the proximal aspect of the capitate to articulate with the scaphoid and the ulnar facet of the distal lunate (Figure 2.5).

Figure 2.4 – Wrist radiograph with a type 1 lunate. Note the large radius of curvature of the capitate which articulates with the scaphoid and single facet of the lunate and triquetrum. From – Nakamura et al., 2000.

Figure 2.5 – Wrist radiograph with a type 2 lunate. Note the small radius of curvature of the capitate. Which articulates with the scaphoid and the radial facet of the lunate but not the ulnar aspect of the lunate or triquetrum. From – Nakamura et al., 2000.

Moritomo reported that the distal scaphoid had a variable articulation with the trapezium and trapezoid (Moritomo et al., 2000; Moritomo et al., 2000). In 81% of cases the distal scaphoid had a distinct facet for the trapezium and the trapezoid, which was separated by a ridge.

The work described in “Scaphoid variation and an anatomical basis for variable carpal mechanics” was the PhD thesis of Quentin Fogg, which was performed under my supervision (Fogg, 2004). The study included an assessment of dry bones and gross cadaveric dissections. This work identified two types of scaphoid, namely a rotating and a flexing scaphoid, with variations in the scaphoid osteology and ligament attachments between the two scaphoid types (Figure 2.6).

NOTE: This figure is included on page 14 of the print copy of the thesis held in the University of Adelaide Library.

Figure 2.6 – Histological view of the carpus including the scapho-lunate ligament. From - Fogg, 2004.

The rotating scaphoid had one dorsal osseous ridge for the radioscaphoid (RS) ligament (Figure 2.7a). In contrast, the flexing scaphoid had three dorsal ridges to also include attachments for the radioscaphocapitate (RSC) and dorsal intercarpal (DIC) ligament (Figure 2.7 b). The different ligament attachments either restrain flexion or rotation of the scaphoid depending upon their position (Figure 2.8, Figure 2.9).

NOTE: This figure is included on page 15 of the print copy of the thesis held in the University of Adelaide Library.

Figure 2.7a,b – Dorsal view of a right scaphoid. With the rotating scaphoid there is a single dorsal ridge for insertion of the radioscaphoid (RS) ligament. In the flexing scaphoid there are 3 ridges for insertion of the radioscaphocapitate (RSC) and dorsal intercarpal ligament (DIC). The middle ridge is for attachment of the radioscaphoid (RS) ligament. Adapted from – Fogg, 2004.

NOTE: This figure is included on page 16 of the print copy of the thesis held in the University of Adelaide Library.

Figure 2.8 – Lateral 3-D views of right scaphoid looking from the radial aspect. In the rotating scaphoid (left) the radioscaphoid (RS) ligament attaches to the dorsal ridge of the scaphoid. The radiocapitate (RC) and dorsal intercarpal ligament (DIC) bypass and encircle the scaphoid. These act like a pulley and help control the position of the scaphoid but allow rotation. In contrast, in the flexing scaphoid (right), the radioscaphocapitate (RSC) ligament attaches to the scaphoid as does the dorsal intercarpal ligament (DIC) and act as rotatory restraints but allow flexion. From – Fogg, 2004.

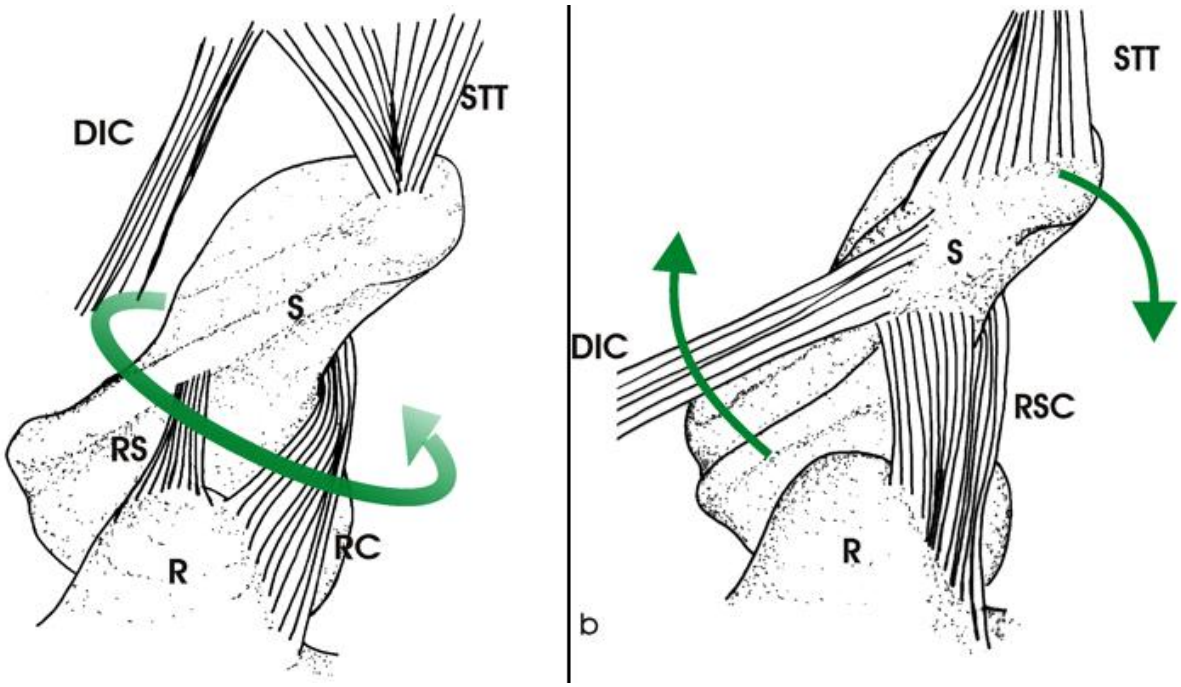

Figure 2.9 – Diagrams of a left scaphoid looking from the radial aspect. Stylised diagram of the rotating and flexing scaphoid. Note in the rotating scaphoid that the dorsal intercarpal ligament (DIC) and radioscaphocapitate (RSC) do not attach to the scaphoid but act as a pulley. The volar scapho-trapezo-trapezoidal (STT) ligament has a narrow base on the scaphoid, which helps to act as a point of rotation around which the scaphoid rotates. In contrast with the flexing scaphoid, the STT ligament has a wide base on the scaphoid. The radioscaphocapitate ligament (RSC) has an attachment to the scaphoid waist, over which it flexes.

In the rotating scaphoid the RSC and DIC ligaments do not attach to the scaphoid but do act as a pulley to stabilise it (Figure 2.10, Figure 2.8). In the flexing scaphoid the RSC and DIC ligaments attach to the scaphoid and restrain rotation, but allow flexion of the scaphoid over the RSC ligament.

NOTE: This figure is included on page 18 of the print copy of the thesis held in the University of Adelaide Library.

Figure 2.10 – Dorsal cadaveric dissection of a left scaphoid. In the rotating scaphoid the dorsal intercarpal ligament (DIC) has a loose membranous (M) attachment to the scaphoid before passing onto the trapezium (Tm). In contrast in the flexing scaphoid the DIC has a strong attachment to the scaphoid and does not extend to the trapezium. From – Fogg, 2004.

Fogg made a number of anatomical observations about the differences of the mid-carpal joint with the type 1 and type 2 lunates. In the wrist with a type 1 lunate there is a large condyle of the capitate with a smooth transition to the hamate (Figure 2.11). The lunate can slide on the capitate without directional restraint. This is a unicondylar joint similar to the hip joint. In contrast, the mid-carpal joint with a type 2 lunate has features of a bicondylar joint that is similar to the knee joint (Figure 2.12). When the hamate is engaged on the lunate, the mid-carpal joint must move in only the flexion/extension arc, as the groove of the lunate is locked into the interval between the capitate and hamate.

NOTE: This figure is included on page 19 of the print copy of the thesis held in the University of Adelaide Library.

Figure 2.11 – Cadaveric coronal section of a right wrist. Type 1 lunate which articulates with a unicondylar mid-carpal joint. This is similar to a hip joint. From – Fogg, 2004.

NOTE: This figure is included on page 19 of the print copy of the thesis held in the University of Adelaide Library.

Figure 2.12 – Cadaveric coronal section of a right wrist. Type 2 lunate with a radial facet which articulates with the capitate and the ulnar facet which articulates with the hamate. This creates a bicondylar mid-carpal joint which is similar to a knee joint. From – Fogg, 2004.

In the wrist with a type 2 lunate the proximal ridges of the capitate and hamate coincide with the radial and ulnar borders of the lunate (Fogg, 2004). Those articular restraints force the mid-carpal joint to act only in a flexion and extension arch. It does not allow translation or rotation. This is quite different to the mid-carpal joint with a type 1 lunate, which does not have these restraints and so behaves more like a universal joint.

Craigen and Stanley demonstrated a spectrum of scaphoid kinematics ranging from column to row mechanics (Craigen and Stanley, 1995). This was based on the relative flexion/extension and translational motions measured on plain AP radiographs. Column kinematic wrists have significant flexion of the scaphoid with radial deviation and minimal translation. In contrast, row kinematic wrists have minimal scaphoid flexion with radial deviation and greater translation. This was quantified using the carpal ratio (CR) index and translation ratio (TR). The authors identified a spectrum of variability, with some wrists having kinematic properties of a row wrist at one end of the spectrum and other wrists having properties of a column wrist at the other end of the spectrum.

Garcia Elias et al. used the same primary data points as published by Craigen and Stanley to compare the relationship between the degree of joint laxity and scaphoid kinematics during radio-ulnar deviation of the wrist (Craigen and Stanley, 1995; Garcia-Elias et al., 1995). Their findings reaffirmed the spectrum of normal kinematics (Figure 2.13) and the row and column theory as reported by Craigen and Stanley. They developed a number of indices to further assess the row and column theory (Figure 2.14). The details of the measurements and calculations have not been reproduced, however these relevant to the studies undertaken are summarised in section 3.1, 3.2.

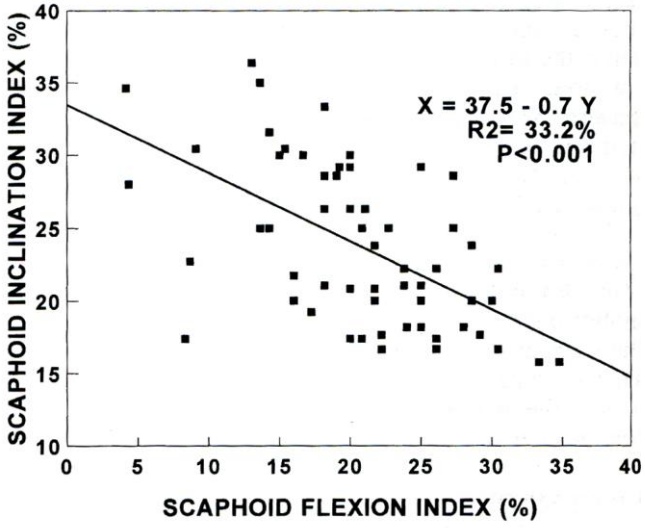

Figure 2.13 – Correlation of scaphoid inclination index to scaphoid flexion index. From - Garcia-Elias et al., 1995.

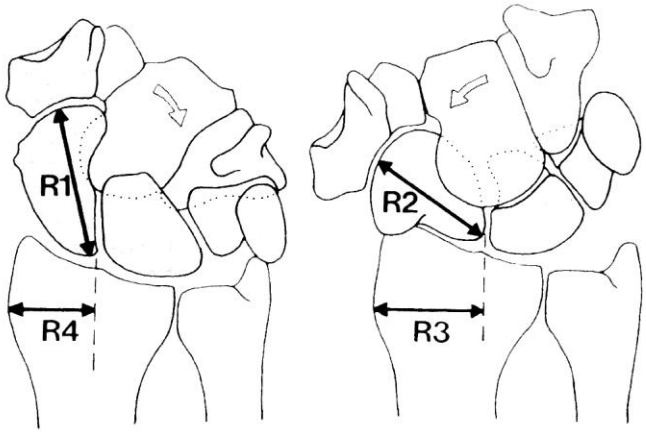

$$\text{Scaphoid Flexion Index: SFI} = \frac{(R1 - R2) \times 100}{R1}$$

$$\text{Scaphoid Inclination Index: SII} = \frac{(R3 - R4) \times 100}{R3}$$

$$\text{Scaphoid Kinematic Index: SKI} = \frac{SFI}{SII}$$

Figure 2.14 – Radiographic measurements obtained in order to calculate the scaphoid indices: From - Garcia-Elias et al., 1995.

The study of carpal kinematics has evolved as advances in computed tomography (CT) and magnetic resonance imaging (MRI) have allowed in-vitro (Berger, 1982; Garcia-Elias et al., 1989; Ruby et al., 1988) and in-vivo (Feipel and Rooze, 1999; Moojen et al., 2003; Wolfe et al., 2000) investigation of three-dimensional carpal kinematics. Despite these advances, there remains uncertainty and debate regarding the movements of the carpus. Carpal kinematic theories have evolved to incorporate several theories on carpal kinematics in addition to those that support the column (Navarro, 1921; Taleisnik, 1976) and row (von Bonin, 1929). This includes the intercalated segment (Landsmeer, 1961; Weber, 1984) and oval ring concepts (Lichtman et al., 1981; Moritomo et al., 2006).

The study on scaphoid kinematics presented in the thesis, aims to address a deficiency in the knowledge between morphology and kinematics of the wrist. It aims to identify the association between the lunate morphology and the scaphoid kinematics.

2.1.3 Triquetro-hamate joint

In 1907 Johnston described the triquetro-hamate (TqH) as a saddle joint with both the hamate and triquetral articular surfaces having concave and convex parts (Johnston, 1907), the convex parts being congruent with the concave parts on the opposite surface (Kauer, 1986). The convex part of the hamate always fits the concave part of the triquetrum, whereas the concave part of the hamate does not fit with the triquetrum except at the ulnar extreme position of the triquetrum (McLean et al., 2006).

Later descriptions have focused on the hamate and have described the hamate surface as helicoid or screw shaped in configuration (Weber, 1984). Similarly, MacConaill described the hamate as having a screw surface that fits the opposite, female surface of the triquetrum (MacConaill, 1941). In both descriptions the facet on the hamate has a dorsopalmar groove that is wound in a spiral fashion. This spiral groove contributes to the helicoidal movement of the triquetrum in relation to the hamate (Kauer, 1986; Weber, 1984). As a result of the spiral groove of the hamate, the triquetrum swerves in the transverse plane during dorsopalmar displacement of the hamate to the triquetrum.

More recently, however, Morimoto et al have proposed that the TqH may not be a saddle joint after all (Moritomo et al., 2003). They contend that the convex part of the hamate forms part of an oval (ellipsoid) joint and that its typical motion is not helicoidal but rotational. In this concept TqH motion is oriented obliquely to the sagittal plane of the wrist. It is described in an ulnar flexion/radial extension motion plane in radioulnar inclination and in an almost flexion-extension plane of motion in flexion-extension inclination of the wrist.

Regarding the joint structure, Burgess described a cup that was formed by the scaphoid, lunate and triquetrum (Burgess, 1990). He observed the difference in vertical alignment of the TqH and suggested a possible relationship between anatomic variation and mid-carpal instability.

In reference to the TqH joint, Johnston described the saddle as appearing irregularly shaped, but since that time few articles in the literature have considered this joint (Johnston, 1907). Burgess acknowledged the variation in the helical surface of the hamate (Burgess, 1990).

Several investigators have examined the relative anatomic motion of type 1 and type 2 lunate wrists (Moritomo et al., 2003; Nakamura et al., 2000; Viegas, 1990) and have attempted to

explain TqH joint motion in terms of these differences; however, there remains much debate as to the exact nature of carpal kinematics.

The study on the triquetro-hamate joint presented in the thesis aims to determine the morphology of this joint. To postulate the kinematic consequences of the morphological factors identified.

2.2 Imaging

2.2.1 Introduction

The second group of papers deals with imaging of the wrist. The rationale for the studies was that there were important gaps in the knowledge. For example, how to perform the CT scan of the scaphoid? How to assess the scaphoid deformity? How to pre-operatively template the fracture to correct the deformity?

The final paper in the imaging chapter deals with portable operative fluoroscopy and assesses what is its role in upper limb surgery.

The studies performed in the thesis sought to address these deficiencies. The literature reviewed encompasses scaphoid fractures and methods of imaging of the wrist. It specifically deals with assessment of scaphoid deformity and CT of the scaphoid. It concludes with a review of fluoroscopy.

2.2.2 Scaphoid fractures

Scaphoid fractures are the most common fractures of the carpus, accounting for 79% of all carpal fractures (Green, 1993). Scaphoid fractures are commonly seen in the young and healthy and are rarely seen in children or the elderly, where a fracture to the distal radius more frequently occurs (Amrami, 2005). Early diagnosis of scaphoid fractures is imperative owing to potential fracture complications including non-union, avascular necrosis, carpal instability and osteoarthritis. There have been many advances in imaging of the wrist in recent years that have vastly increased the ability to identify and assess scaphoid fractures.

Seventy per cent of all scaphoid fractures are through the waist, 20% involve the proximal pole, with the remaining 10% involving the distal pole. The prognosis of the distal fracture is better than that for proximal fracture, primarily owing to the nature of the retrograde blood supply to the scaphoid (Gelberman et al., 1983). Subsequently the time required for healing

also varies according to fracture location, with distal fractures often healing within four to six weeks, while waist and proximal pole fractures may require six to eight weeks, if indeed they will ever unite (Plancher, 2001).

2.2.3 Plain radiography

Plain radiography has been the mainstay of scaphoid imaging for the last one hundred years. However, it is less than optimal for the evaluation of scaphoid fracture, union and deformity, due to the poor resolution provided by plain radiography (Biondetti et al., 1987; Engdahl and Schacherer, 1989; Friedman et al., 1990). Dias reported that experienced observers will report a scaphoid fracture in 20% of normal asymptomatic wrists (Dias et al., 1990).

A Meta-analysis of several large series has shown that scaphoid fractures are initially radionegative in around 16% of cases (Hunter et al., 1997). Fractures can also take up to 1 to 2 weeks to become evident on plain film. Eighty four per cent of patients undergo an unnecessary immobilization in a plaster cast for an extra two weeks, with the subsequent lifestyle, working and dressing restrictions, during which time the patient still does not know if the scaphoid is fractured. Studies have reported that repeat plain radiographs have a poor interobserver reliability coefficient (Landis and Koch, 1977; Low and Raby, 2005; Tiel-van Buul et al., 1992; Tiel-van Buul et al., 1993).

The scaphoid fat stripe is seen on PA and oblique views as a thin lucent line paralleling the lateral border of the scaphoid bone with a slight convexity towards it. It is postulated that trauma to the scaphoid may result in blood and oedema accumulation subsequently altering the configuration of this fat stripe (Annamalai and Raby, 2003; Terry and Ramin, 1975). However, Annamalai et al reported only 50% correlation between MRI confirmed scaphoid fractures and the presence of the scaphoid fat stripe (Annamalai and Raby, 2003).

Specific radiographical methods of performing plain radiography have been reported. Techniques have included the carpal box technique (Proubasta et al., 1989), panoramic x-rays of the carpus (Berna et al., 1993) and macro radiography (Gaebler et al., 1998).

Fernandez described a method of pre-operative templating of scaphoid fractures using tracing paper on plain radiographs (Fernandez, 1984). However the author has found this difficult to perform due to the poor resolution of the scaphoid image with plain radiographs. This is compounded by the adjacent carpal bones which overly the scaphoid in the lateral projection,

which makes interpretation difficult. In addition the plane of the images is oblique to the natural alignment of the scaphoid. Therefore the author set out to identify a method that would overcome these difficulties.

2.2.4 Trispiral tomography

When a scaphoid fractures it can have a detrimental effect on the carpal alignments. The fractured scaphoid shortens and the distal scaphoid fragment flexes relative to the proximal fragment. This produces the characteristic "humpback deformity" (Smith et al., 1989; Weber, 1980) (Figure 2.15). Tomography improves imaging and provides a more detailed view of the scaphoid and for this reason has been utilized to assess the scaphoid deformity (Amadio et al., 1989).

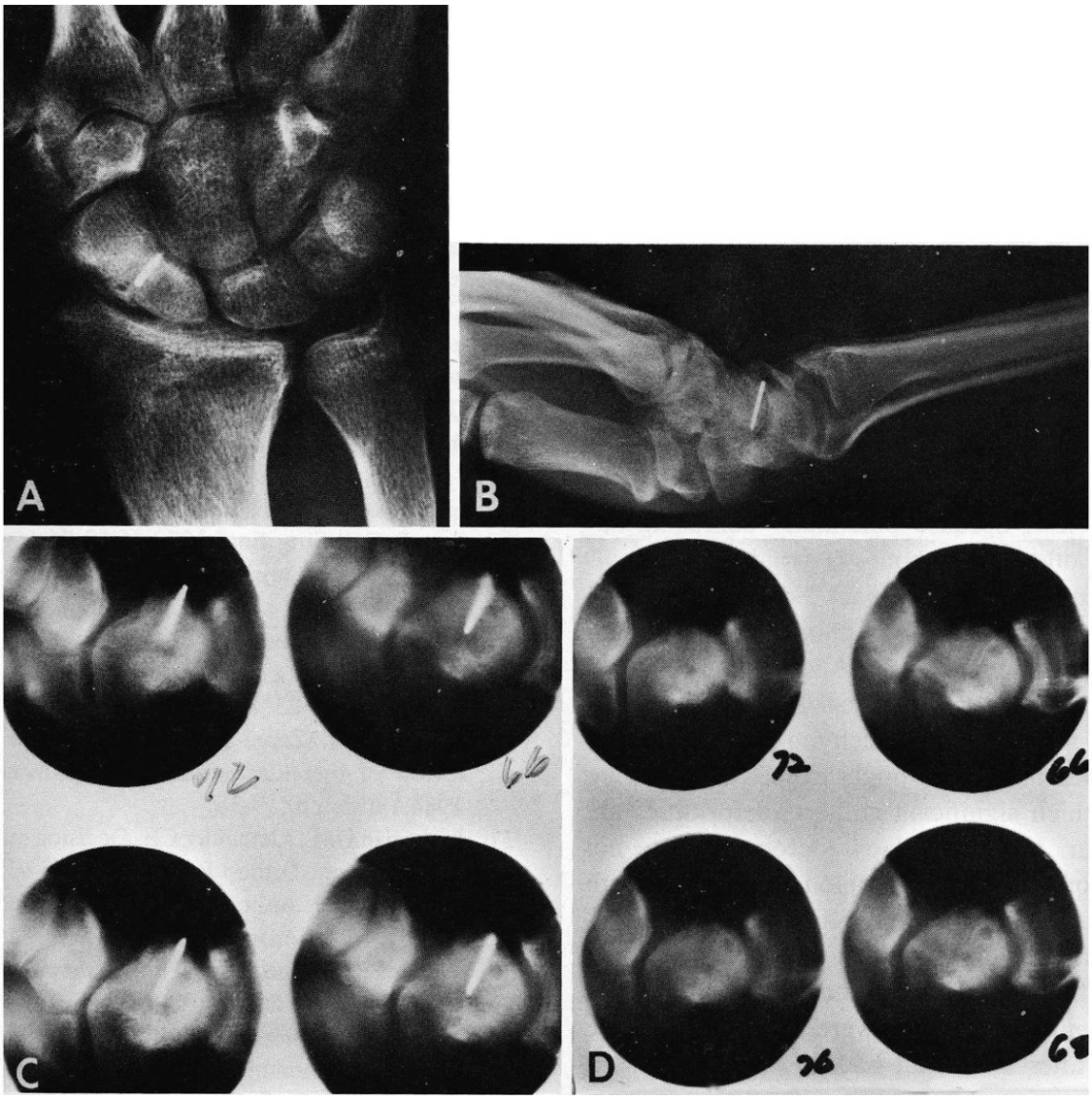

Figure 2.15 – Radiographical views of the right scaphoid. Percutaneous electrical stimulation was used to achieve union in this angulated scaphoid fracture. Seven years later, significant degenerative change associated with pain and limited extension caused the patient to return for re-evaluation. **A**, Anteroposterior view, note retained stimulation wire; **B**, lateral view; **C**, lateral tomogram, note improved detail of scaphoid anatomy; **D**, one year after cheilectomy, patient had improved motion and less pain. From - Amadio et al., 1989.

Amadio et al used lateral Trispiral tomography to measure the lateral intrascaphoid angle (Amadio et al., 1989) (Figure 2.16). He reported that the lateral intrascaphoid angle was superior to the AP intrascaphoid angle, the radiolunate angle and the carpal height ratio in predicting clinical outcome. The scaphoid deformity decreases wrist motion, alters carpal kinematics (Burgess, 1987) and predisposes the patient to progressive pain and degenerative arthritis (Amadio et al., 1989; Birchard and Pichora, 1990; Mack et al., 1984; Nakamura et al., 1991; Ruby et al., 1985; Vender et al., 1987).

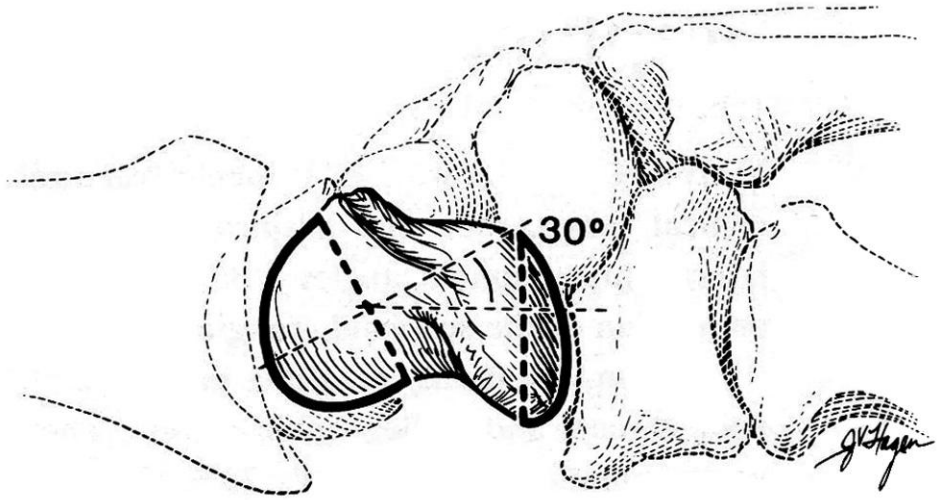

Figure 2.16 - Intrascaphoid angle. Lateral diagram of left wrist. A perpendicular line is drawn to the proximal and distal articular surfaces and the resulting angle is measured. From - Amadio et al., 1989.

The assessment of scaphoid deformity with the intrascaphoid angle can be difficult when using plain radiographs or Trispiral tomography. The study on the measurement of the humpback deformity aims to assess the reliability of the intrascaphoid angles and compare it to other new methods of assessment of scaphoid deformity.

2.2.5 Bone scintigraphy

Bone scintigraphy is performed following intravenous injection of ^{99m}Technetium disphosphonate ($^{99}Tc^{m}$-MDP). This phenomenon arises from the affinity of technetium for areas of increased osteoblastic activity or hyperaemia and is observed following a fracture or any other osseous abnormality of the skeleton (Duncan and Thurston, 1985).

Tiel-van Buul et al reported only moderate intra-observer and inter- observer agreement of the early bone scan images (kappa values of approximately 0.5), which was thought to be due to difficulty of adequate localization of the hotspot (Stordahl et al., 1984; Tiel-van Buul et al., 1992). Tiel-van Buul also reported a positive predictive value of 94% (Stordahl et al., 1984; Tiel-van Buul et al., 1992). Other authors have reported bone scintigraphy sensitivities approaching 100% (Stordahl et al., 1984; Vrettos et al., 1996). However, false positives (up to 25% when compared with delayed radiographs) and decreased specificity varying between 60 and 95% with the use of bone scintigraphy (Bayer et al., 2000; Fowler et al., 1998; Gaebler et al., 1996; Hambidge et al., 1999; Tiel-van Buul and et.al, 1997). This is due to increased uptake from other traumatic conditions such as scapho-lunate instability, bone bruises, synovitis and arthritis (Rolfe et al., 1981).

Other limitations include that it is an invasive procedure that exposes the patient to a low dose of radiation and is contraindicated in pregnancy (Amrami, 2005). Because delay in activation of the osteoblast, a bone scan will initially be negative and does not reach maximal predictive power until 72 hours following the injury. In elderly or debilitated patients this may be delayed 7-10 days because of the delay in osteoblastic activity (Belsole et al., 1981).

A negative bone scan rules out a scaphoid fracture which is why it had been popular. A positive scan does not diagnose a fracture but often requires further investigation (e.g. longitudinal CT scan) to confirm a fracture.

Quantification bone scanning involves assigning numerical values to the degree of $^{99}Tc^{m}$-MDP uptakes in hot spots. In an attempt to determine the significance of a hotspot, Groves et al identified scaphoid fractures that were diagnosed on bone scan and performed quantification of $^{99}Tc^{m}$-MDP in these lesions (Groves et al., 2005). Overall greater values were recorded in CT confirmed scaphoid fracture than other lesions such as a “bone bruise” (Rangger et al., 1998; Resnick and Georgen, 2003).

2.2.6 High spatial resolution sonography

High spatial resolution sonography (HSRS) has been reported for diagnostic purposes, with the transducer operating between 5 to 15 MHz (Fusetti et al., 2005; Hodgkinson et al., 1993). However, these have not become popular owing to user variability and the fact that the treating clinician does not have the ability to read the ultrasound images.

2.2.7 Computed tomography

Computed tomography (CT) is increasingly utilized as the definitive investigation for the management of scaphoid fractures (Engdahl and Schacherer, 1989; Jonsson et al., 1992; Quinn et al., 1987; Sanders, 1988; Smith et al., 1989; Wilson et al., 1990). Imaging along the longitudinal axis is most suitable for the evaluation of scaphoid fractures and healing (Jonsson et al., 1992; Sanders, 1988; Wilson et al., 1990). Various techniques for CT imaging along the longitudinal scaphoid axis have been described, (Biondetti et al., 1987; Quinn et al., 1987; Smith et al., 1989) most of which require the wrist to be positioned in ulnar deviation, or which require the use of an immobilization device. Many patients with scaphoid fractures find this position uncomfortable and move during scanning despite attempts at immobilization. It was not uncommon for the image obtained to be oblique to the longitudinal plane, which makes interpretation of deformity more difficult. With the various described techniques the assessment of the scaphoid morphology and appreciation of the deformity has been difficult.

The study on the longitudinal computed tomography of the scaphoid aims to address a deficiency in the knowledge of how to image the scaphoid and to provide a standardised method that will allow a better comparison so that the abnormal morphologies can be better appreciated.

Moritomo et al reported that the fracture location in scaphoid non-union affected the pattern of deformity (Moritomo et al., 2000). The fracture location was measured based on the anatomical landmark of the dorsal apex of the scaphoid ridge where the proximal part of the dorsal intercarpal ligament and the dorsal scapho-lunate interosseous ligament attach. Fractures which occurred distal to the dorsal apex of the ridge developed a humpback deformity. Fractures proximal to this ridge did not.

Oka et al analysed 24 patients known to have established non-union (Oka et al., 2005). The patients were divided into two groups based on the Moritomo classification (Moritomo et al., 2000), using 3D CT modelling. To assess the size and shape of the scaphoid defect, the scaphoid was reconstructed and compared to the contralateral scaphoid, which was used as a template. The distal scaphoid fractures, all displayed a wedge-shaped bone defect with a volar base. The mean volume loss was 9% of the contralateral normal scaphoid. In contrast, proximal scaphoid fractures had a flat, crescent-shaped defect that represented 1% of the contralateral scaphoid. The size of bone defect was not significantly different between the

short duration and the long duration fractures (Oka et al., 2005). In proximal fractures, ligamentous attachments remain on the distal fragment and therefore maintain stability of the distal fragment. However, in distal scaphoid fractures the fracture is beyond the ligament attachment and therefore cannot resist flexion forces generated by axial loads, resulting in a humpback deformity. A distal scaphoid non-union tends to display symptoms earlier than a proximal non-union because of the greater bone deformity and subsequent carpal instability.

2.2.8 Magnetic resonance imaging

Magnetic resonance imaging (MRI) scans have become more commonly used for the assessment of the acutely injured wrist. The American College of radiology (Rubin, 2005) has established an appropriateness criterion for initial investigation of the acute wrist injury. The college has issued a score of 8 out of 9 for the use of early non-contrast MRI as an imaging modality in a suspect acute scaphoid fracture with normal initial radiographs. The advantage of MRI is its ability to detect occult fractures of the scaphoid and carpus, and also soft tissue injuries. Other associated injuries can be identified including a distal radial or capitate fracture and tears of the scapho-lunate ligament and triangular fibrocartilage (Mack et al., 2003).

However, once a fracture is confirmed, the CT scan is the preferred imaging modality as it provides a better appreciation of the morphological changes.

MRI has been reported to have excellent sensitivity (100%) and specificity (95-100%) for assessment of acute fractures (Breitenseher et al., 1997; Gaebler et al., 1996; Hunter et al., 1997). MRI can detect fractures of the scaphoid although it can be difficult to differentiate from bone bruising (Brydie and Raby, 2003; Mack et al., 2003). A negative aspect of MRI imaging is that claustrophobia is experienced by 1-30% of patients (Avrahami, 1990; Kilborn and Labbe, 1990).

Several groups have recently looked into the cost-effectiveness of early MRI in comparison to the historically traditional protocol of repeat plain radiographs at 10-14 days for detecting scaphoid fractures (Brooks et al., 2005; Dorsay et al., 2001; Gooding et al., 2004; Kukla et al., 1997). When lost productivity and income to the patient are considered, early MRI is favoured at initial presentation compared to performing repeat plain radiographs at two weeks (Brooks et al., 2005; Dorsay et al., 2001; Gooding et al., 2004).

2.2.9 Fluoroscopy

Fluoroscopy has been used in the kinematic assessment of carpal instability (Braunstein et al., 1985; Protas and Jackson, 1980; White et al., 1984).

Intra-operative fluoroscopy was first described by Coltman in 1984 and has since been used extensively in operative procedures. Plain radiographs have been recommended following arthroscopic "ectomy" procedures to ensure that an adequate bony resection has been performed (Roth and Poehling 1990). Advances in fluoroscopic technology have enabled high-resolution images to be obtained using significantly lower radiation exposure (Gehrke et al., 1993). Their role has been defined in the foot and ankle, but not reported in the upper limb surgery (Gehrke et al., 1993). The study on portable operative fluoroscopy aims to determine the role of fluoroscopy in the surgical management of disorders of the upper limb surgery.

2.3 Arthroscopy

2.3.1 Introduction

The third group of papers deals with arthroscopy of the wrist. The rationale for the studies was that there were important gaps in knowledge in these areas; therefore the studies performed in the thesis sought to address these deficiencies. The literature reviewed encompasses all areas of wrist arthroscopy. It specifically deals with arthroscopy for the following conditions, Kienböck's disease, and fracture of the distal radius, STT joint arthritis, intra-osseous ganglion of the lunate, wrist contracture and ulnar stylo-carpal impaction.

2.3.2 Historical perspectives

Professor Kenji Takagi first reported arthroscopy in 1920. In the 1970s arthroscopy of the knee had become quite popular and progressed from a diagnostic to a therapeutic procedure. But it was not until 1979, when small joint arthroscopy was adequately developed, that Yung-Cheng Chen first described the procedure in the wrist (Chen, 1979). However, wrist arthroscopy did not become a common diagnostic or therapeutic modality until an instructional course lecture in 1986 was provided at the American Academy by doctors Roth, Poehling and Whipple (Roth et al., 1988). The introduction of arthroscopic instrumentation has enabled therapeutic arthroscopy to become efficiently performed (Roth 1988b). Two decades later wrist arthroscopy has developed into an accepted diagnostic and therapeutic

tool. The practice of arthroscopy has been extended as the principles of open surgical procedures have been adapted to the arthroscopy.

2.3.3 Comparison of diagnostic arthroscopy to imaging modalities

Arthrography

Arthrography is an injection into an anatomical space followed by radiographs. It is aimed to assess if there is a leakage of contrast from one space to another, therefore it assesses if there is containment of the contrast in the compartment.

Wrist arthroscopy has been reported to be superior to radiocarpal arthrography in providing anatomical information and diagnostic accuracy within the wrist joint (Roth and Haddad, 1986). These results were compared to an open arthrotomy, which was used as the gold standard.

Comparison of 3-compartment arthrography with arthrotomy revealed a false-positive rate from 10 to 20 per cent (Levinsohn et al., 1987).

There may be false-negative results due to perforations obstructed by synovitis or fibrosis. A tear may act as a flap valve and prevent communication of contrast between compartments. Arthrography does not quantify the size or type of the perforation or its biomechanical consequence on the wrist. An extensive tear and a small perforation may have the same arthrographic appearance. Arthrography does not provide adequate information about adjacent structures such as the articular cartilage and synovium. Herbert reported on a series of bilateral wrist arthrograms in which 74% had a positive arthrogram on the contralateral, asymptomatic wrist (Herbert et al., 1990).

In contrast, arthroscopy provides detailed anatomic information. Palpation with the arthroscopic probe allows assessment of the stability and texture of intra-articular structures and measurement of defects. The stability of ligaments can be assessed under direct vision while the joint is stressed with a probe or by external manipulation. The adjacent structures such as the synovium and articular cartilage can be clearly seen, allowing a more thorough assessment of the wrist. The surgeon can then treat the abnormalities that are seen.

Magnetic resonance imaging

MRI is a non-invasive diagnostic modality that has the advantage of also being able to image the soft tissues of the wrist. MRI can distinguish triangular fibrocartilage complex (TFCC) degeneration from perforation (Kang et al., 1991). Sensitivity rates for diagnosis of TFCC tears range from 72 to 93%, which are similar to the sensitivity rate reported for conventional radiocarpal arthrography but less than that for 3-compartment arthrography (Gundry et al., 1990). MR imaging produces false-negative images. However there are generally only a few false-positives. False-positive images are due to irregularities of the central portion of the TFCC.

MRI is has been poor at identifying detects in the cartilage (Cerofolini et al., 1990; Kang et al., 1991). Cerofolini and colleagues reported that in none of their 10 cases was MR imaging able to visualize cartilaginous lesions later seen at arthroscopy (Cerofolini et al., 1990). However, with improved techniques such as the use of dedicated wrist coils and intra-articular gadolinium, the resolution has improved for the assessment of chondral defects and interosseous ligament tears (Kato et al., 2000) (Potter et al., 1997).

2.3.4 Indications for arthroscopy

The indications for arthroscopy can be considered as diagnostic and therapeutic. Table 2.1 provides a list of indications for wrist arthroscopy written by the author in 1994, at the commencement of the thesis, and subsequently published in 1996 (Bain et al., 1996).

Table 2.1 – Indications for Wrist Arthroscopy 1996

Diagnostic arthroscopy	Assessment of ligamentous injuries of the wrist
	Scapho-lunate ligament disruption
	Lunotriquetral ligament disruption
	TFCC disorders
	Assessment of chondral defects
	Assessment of chronic wrist pain of unknown etiology
Therapeutic arthroscopy	[1]ARIF of scapho-lunate and lunotriquetral ligament tears
	[1]ARIF of distal radial fractures
	Debridement and repair of TFCC tears
	ARIF of scaphoid fractures
	Lavage of septic arthritis
	Synovectomy
	Removal of loose bodies
	Debridement of chondral defects
	Debridement of degenerative arthritis
	Excision of ganglion
	Resection arthroplasty
	Distal ulnar resection

[1]ARIF - Arthroscopic assisted reduction and internal fixation;
TFCC triangular fibrocartilage complex.
From – Bain et al., 1996.

2.3.5 Instrumentation

The initial instruments for wrist arthroscopy were hand-held manual cutting instruments. Motorised resectors have become popular as they are more efficient than manual cutting instruments (Whipple, 1988). The full-radius resectors are often used for small joint arthroscopy because they provide a larger aperture. Motorised resectors work most efficiently at low speeds, such as 400 rpm (Whipple, 1988). At higher speeds there is insufficient time for the soft tissue to enter the cutting mechanism, effectively closing the aperture (Whipple, 1988). The 3.5mm full-radius resector is used in the radiocarpal joint and the 2mm resector in the mid-carpal joint.

Motorized burs are effective for removing bone. It is best to use the suction intermittently to clear debris, because with continuous suction, the bone swirls in the turbulence and restricts visibility. Burs perform best in bone at high speeds such as 1200 rpm (Whipple, 1988).

The improvement in instrumentation has been important as it has allowed the surgeon to extend the indications of wrist arthroscopy to include more complex therapeutic procedures (Roth and Poehling, 1990; Whipple, 1992).

2.3.6 Technique of wrist arthroscopy

General or regional anaesthesia is preferred by most authors (Ruch and Poehling, 2005) although local anaesthetic techniques have also been reported (Ho, 2007). The patient is supine, with the shoulder along the edge of the operating table (Figure 2.17). A tourniquet is placed above the elbow and inflated to 250 mmHg. The shoulder is abducted 70-90 degrees and the forearm is suspended vertically (using finger traps) from a wrist tower, shoulder arthroscopy frame or an articulating arm attached to the operating table. A sling with a 5kgs weight is placed over the tourniquet to provide downwards counter-traction and thus distraction of the wrist joint. There have also been descriptions of arthroscopy in which the arm is placed on a hand table and traction applied via finger traps, with a weight over the side of the arm table.

Figure 2.17 – Photograph of operating room set-up for performing wrist arthroscopy. The wrist is suspended via finger traps from a shoulder frame. Image from private file.

A 2.5mm scope is used with a 30-degree viewing angle. A short bridge arthroscope (lever arm of 100mm) allows for easier control. The wrist is examined and landmarks are palpated (Table 2.2). Marking the surface anatomy and portals until the surgeon is experienced in portal placement is recommended.

Table 2.2 - Arthroscopic Wrist Portals

Portals	Technique	Comment
Radio-carpal Dorsal Portals		
1-2	Inserted in the extreme dorsum of the snuffbox just radial to the EPL tendon to avoid the radial artery. (Abrams et al., 1994).	Gives access to the radial styloid, scaphoid, lunate and articular surface of the distal radius.
3-4	The portal is 1cm distal to Lister's tubercle between the tendons of the third and fourth compartment.	Main working portal. Gives a wide range of movement and view.
4-5	In between the common extensor 4th compartment and EI in the 5th compartment.	Usually the 6R portal is used in preference.
6R	Located distal to the ulna head and radial to the ECU tendon. This portal is established under the direct vision of the arthroscope using a needle. This avoids damage to the TFCC.	Main working portal.
6U	Established under direct vision similar to the 6R portal. Always blunt dissection to avoid the dorsal branches of the ulna nerve.	6U and 6R portals allow visualisation back towards the radial side and access to the ulna-sided structures.
DRUJ	Forearm supinated to relax dorsal capsule. Arthroscope introduced into axilla between radius and ulna underneath the TFCC.	Gives a view of the DRUJ articulation.
Mid-carpal Portals		
MCR	Soft depression palpated between proximal and distal carpal rows. 1cm distal to the 3-4 portal along a line bordering the radial edge of the 3rd metacarpal.	Can use this to visualise the STT joint, scapho-lunate articulation and distal pole of scaphoid.
MCU	Soft depression palpated between the proximal and distal carpal rows 1 cm distal to 4-5 portal inline with the 4th metacarpal.	Allows visualisation of distal lunate, lunotriquetral and triquetral hamate articulation.
STT	Between EPL and ECRB in the mid-carpal row. On the ulnar margin of the EPL tendon. Terminal branches of the radial sensory nerve at risk.	Used with the MCR portal for STT debridement.
Volar Portals		
VRRC	2cm longitudinal incision overlying FCR on radial side of volar proximal wrist crease. FCR retracted ulnarly. Radiocarpal joint identified with needle then port expanded with artery forceps. An inside-out technique is preferred by the author. Between RSC and LRL ligaments, stay to the radial side of the FCR tendon to avoid the median nerve.	Safe zone of 3mm in all directions with respect to palmar cutaneous branch of median nerve (ulnarly) and radial artery (radially).
VURC	2cm longitudinal incision. FCU identified and retracted ulnarly with the ulna nerve. Interval between FCU and common flexor tendons. Needle inserted into joint then expanded with an artery forcep.	Both volar portals used to assist in reduction of distal radius fracture, view the dorsal articular surface and dorsal ligaments.
VUMC	Volar open approach.	View of the ulnar mid-carpal joint.
DRUJ	Using the same mini-open approach as for VU portal. Care taken to stay below the TFCC.	Gives a view of the DRUJ and deep-sided TFCC tears.

Abbreviations – Extensor Polices Bevis (EPB), Extensor Carpi Radials Longas (ECRL), Extensor Polices Longas (EPL), Extensor Digit rum Commines (EDC), Extensor Indices (EI), Extensor Carpi Ulna is (ECU), Triangular Fibrocartilage Complex (TFCC), Distal Radioulna Joint (DRUJ), Scapho-Trapezium-Trapezoid Joint (STT), Extensor Carpi Radialis Brevis (ECRB), Mid-carpal Radial (MCR), Flexor Carpi Radialis (FCR), Radioscaphocapitate Ligament (RSC), Long Radiolunate Ligament (LRL).

2.3.7 Portals

The radiocarpal portals are numbered according to their relation to the extensor tendon compartments. For example the 1-2 portal is situated between the first and second extensor compartments. An overview of the portals is presented in Table 2.2.

Gravity inflow with lactated Ringers solution is usually utilised, although some authors have recommended a pump(Ruch and Poehling, 2005). From this portal approximately 70% of the radiocarpal joint can be visualised (Ruch and Poehling, 2005).

The ulnar radiocarpal portals allow visualisation of the TFC, triquetrum and pisoform (Ruch and Poehling, 2005).

The DRUJ portal is located by palpating the radial edge of the ulnar head. The wrist is supinated to relax the dorsal capsule and to facilitate entry. The arthroscope can be introduced into the angle between the ulna and radius or just beneath the TFCC. It is easier to insert the scope in the most proximal portal.

A mini open approach is used for the 1-2, 6U, STT portals because of the proximity of the cutaneous nerves. The 1-2 portal is located in the extreme dorsum of the anatomic snuffbox, just radial to the extensor pollicis longus tendon, to avoid the radial artery (Whipple, 1992). It provides access to the radial styloid, scaphoid and articular surface of the distal radius. Its uses include reduction and Kirschner (K) wire fixation of radial styloid fractures as well as insertion of K-wires for pinning of the scapho-lunate interval.

Multiple portals have been described (Figure 2.18) (Abrams et al., 1994) although the 3-4, 4-5, 6R and mid-carpal portals remain the working portals (Culp, 1999; Green et al., 2005).

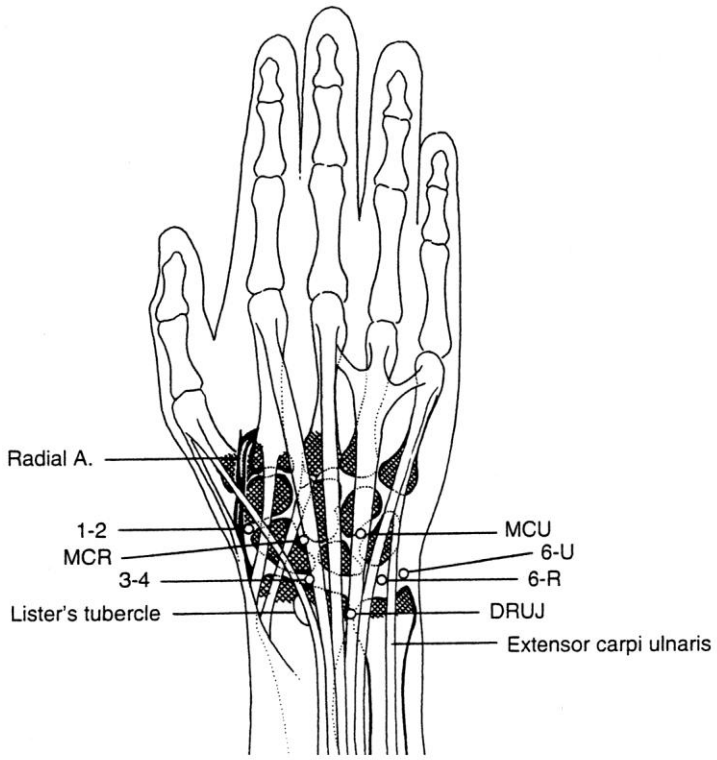

Figure 2.18 - Dorsal wrist arthroscopy portals. The convention is to describe portals according to their anatomic location. The radiocarpal portals are numbered according to their relation to the extensor compartments, e.g. the 3 4 portal is situated between the third and fourth extensor compartments; the 6R compartment is on the radial side (R) of the Extensor Carpi Ulnaris tendon (sixth compartment). A=artery; DRUJ = distal radioulnar joint; MCR = mid-carpal radial; MCU = mid-carpal ulnar. From - Bain et al., 1997.

All arthroscopic examinations of the wrist should include both the mid-carpal and radiocarpal joints (Ruch and Poehling, 2005) as the mid-carpal arthroscopy provides valuable information about the stability and alignment of bones in the proximal carpal row (Geissler et al., 1996).

Many of the advances in wrist arthroscopy have been derived from the development of new portals. Jantea described a volar portal lateral to the radioscaphocapitate ligament (Jantea et al., 1994). Owing to the close proximity of the radial artery this technique did not become popular. Tham reported on using an open volar approach to obtain the portal due to the close proximity of the neurovascular structures (Tham et al., 1999).

Slutsky reported on a clinical and cadaveric study of the use of the radial volar portal (Slutsky, 2002). He used an outside-in technique and reported that it provided a superior view of the dorsal capsule and the volar aspect of the scapho-lunate ligament. He used this portal to identify and repair tears of the dorsal radiocarpal ligament. From his cadaveric study, Slutsky identified the close proximity of the palmar cutaneous branch of the median nerve (3-5mm, average 4mm). He reported that there was a safe zone of 3mm in all directions when performing a volar radiocarpal portal. Via the same open outside-in technique, Slutsky also reported on the use of a volar distal radioulnar joint portal and ulnar mid-carpal portal.

Abe reported that the volar portal was useful for distal radius fractures, particularly when assessing the dorsal rim fractures, assessing volar tears of the scapho-lunate and luno-triquetral ligaments (Abe et al., 2003). He also reported that synovitis on the dorsal aspect of the radiocarpal joint in rheumatoid arthritis can be debrided. They reported that in 230 cases they had not encountered any structural complications.

With the advent of new volar portals, it is now possible to have viewing and working portals that encircle the wrist (Abe et al., 2003; Slutsky, 2002; Tham et al., 1999). This enables the arthroscopic surgeon to view and instrument from all directions. The arthroscope and working portals can be adjusted to obtain the best view and to have the instruments directed into the optimal position to ensure that the therapeutic procedures can be efficiently performed.

2.3.8 Diagnostic arthroscopy

The indications for wrist arthroscopy are both diagnostic and therapeutic.

Initial developments in arthroscopy were to develop an understanding of the normal intra-articular anatomy and to then to expand this understanding of the arthroscopic findings in the injured and diseased wrist.

Arthroscopy provides a great advantage to the surgeon because of the magnification provided by arthroscopy. This enables the surgeon to clearly visualise the intricacies of the intra-articular anatomy and pathology. It is interesting that the volar capsular ligaments are better visualised and understood with arthroscopy then they are with open surgery.

Palpation of the intra-articular structures is an important feature of diagnostic arthroscopy and allows tears of the TFC to be opened to determine the extent of the tear. The probe can be

placed in the scapho-lunate interval in the mid-carpal joint to determine the grade of scapho-lunate instability (Geissler et al., 1996).

Wrist arthroscopy is indicated to confirm findings suggested by other diagnostic modalities or for the diagnosis of wrist pain of unknown etiology. Wrist arthroscopy can be used to assess the severity of degenerative changes prior to other surgical procedures; this would include assessing the mid-carpal joint before proceeding to a proximal row carpectomy or the status of an interosseous ligament prior to reconstruction.

2.3.9 Therapeutic arthroscopy

Having developed an understanding of the diagnostic role of arthroscopy, the next stage was to develop arthroscopy to be used as a therapeutic tool.

The initial arthroscopic therapeutic procedures were "ectomy" procedures (Roth and Poehling, 1990). This involved excision of different intra-articular components of the wrist joint including debridement of synovium, ganglion, removal of loose bodies and debridement of chondral flaps. More advanced techniques have included an excision of bony structures including of the radial styloid, proximal row carpectomy (Roth and Haddad, 1986) and excision of the pisiform (Osterman, 2001).

2.3.10 TFC tears and ulnar carpal impaction

Injury to the TFCC is a common cause of ulnar-sided wrist pain. Wrist arthroscopy has become the gold standard in the diagnosis and treatment of these injuries (Pederzini et al., 1992; Roth and Haddad, 1986). Arthroscopy can assess the tear size and stability as well as any associated synovitis and chondral or ligament lesions.

The TFCC attaches to the sigmoid notch of the distal radius and spans across the ulnar head to attach to the base of the ulnar styloid (Palmer, 1989). The function of the TFCC is both to stabilize (the DRUJ and ulnar carpus) and to transmit load (20% of the total load in ulnar neutral variance) (Palmer et al., 1984). Only the peripheral 25% of the TFCC on the dorsal, volar and ulnar margins is vascularised (Bednar et al., 1991). The central and radial portions remain avascular. Lesions in these areas do not have the potential to heal and are therefore treated with debridement. The dorsal and volar ligaments (peripheral 2mm) maintain stability of the TFCC and it is crucial that these be preserved (Adams, 1993).

Palmer's classification of TFCC injuries can be used to help guide treatment (See Table 2.3) (Palmer, 1989). This divides lesions into type 1 (traumatic) and type 2 (degenerative). Type 1 lesions are classified according to the location of the tear.

Table 2.3 - TFCC Injuries – Palmer's Classification.

Type of Tear	Description of Tear
Traumatic	
1A	Tear in horizontal or central portion of disc.
1B	Tear from distal ulnar insertion ± ulnar styloid fracture.
1C	Tear with ulnocarpal ligaments disrupted. (Ulnolunate and Ulnotriquetral ligaments).
1D	Tear from radial insertion
Degenerative	
2A	TFCC wear but no perforation
2B	TFCC wear but no perforation - Chondromalacia of lunate or ulnar head
2C	Central perforation of TFCC - Chondromalacia of lunate or ulnar head
2D	Central perforation of TFCC - Chondromalacia of lunate or ulnar head - Perforation of LT ligament
2E	Central perforation of TFCC - Perforation of LT ligament - Ulnocarpal arthritis

Abbreviations -

Triangular fibrocartilage complex (TFCC), Flexor carpi ulnaris (FCU), Extensor carpi ulnaris (ECU), Lunotriquetral ligament (LT). From - Palmer, 1989.

Central tears (Type 1A) are managed with arthroscopic debridement of the TFCC tear, performed with the arthroscope in the 6-R portal and the instruments in the 3-4 portal. The 3.5mm oscillating resector removes degenerative fibrocartilage and adjacent synovitis. The outcomes from this limited debridement are rewarding with 80-85% of patients requiring no further surgery and having a good to excellent result (Gan et al., 1995; Whipple and Geissler, 1993). In those patients where there is a neutral or negative ulnar variance, arthroscopic debridement of the TFC is all that is required. In patients who have positive ulnar variance, additional procedures may be required such as a diaphyseal ulnar shortening.

A peripheral tear in the TFCC (Type 1B) can be difficult to detect. A normal TFCC has tension within its substance when applying a probe across it - referred to as the "trampoline effect". Loss of this normal trampoline effect would indicate that there is a peripheral tear of the triangular fibrocartilage (Hermansdorfer and Kleinman, 1991). Patients with a peripheral tear can be managed with either an outside-in or inside-out repair technique (Poehling et al., 1994; Whipple and Geissler, 1993). Newer techniques using a slotted cannula, suture welding and mini-incisions methods performed with arthroscopic assistance, have also been developed (Badia and Khanchandani, 2007; Culp, 2005; Pederzini et al., 2006).

When an unstable peripheral tear is associated with a fractured ulnar styloid, an open procedure must be performed to address the ulnar styloid fragment either through bony reattachment or fragment excision and reattachment of the TFC to the remaining distal ulna. The ECU tendon sheath is intimately related to the dorsal aspect of the TFCC (Palmer, 1990). A peripheral TFCC tear may be associated with ECU subluxation and require open reconstruction in addition to any arthroscopic procedures performed.

Type 1C lesions involve disruption of the TFCC from the ulnar extrinsic ligament complex. At arthroscopy there will be laxity of the ulnar intrinsic ligaments and the pisiform may be easily identified through the ligament rent. These injuries are less common but more complex to manage (Culp, 2005). Augmentation with a flexor carpi ulnaris distally based strip (which is then brought to the dorsal aspect of the triangular fibrocartilage) can also be performed (Culp, 2005).

Type 1D radial-sided tears have a poor chance of healing. This is due to the relative avascularity of the radial side of the TFCC and the fact that it attaches onto the articular cartilage of the sigmoid notch. The majority of these tears are managed with arthroscopic

debridement; however, a number of suture techniques have previously been published, with two-thirds of patients having good to excellent results (Cooney et al., 1994; Culp, 2005; Sagerman and Short, 1996). Techniques have included using a jig to assist in guiding advancing K-wires or needles from the ulnar side to the radial side of the wrist. Trumble described the use of a cannula and then preloaded meniscal repair sutures (Trumble et al., 1996). This allows pre-placed sutures to be fixed onto the radius.

Type 2 TFCC lesions are degenerative tears that are often asymptomatic (Mikic, 1978). Most symptomatic degenerative tears of the TFCC are related to chronic overloading of the ulnocarpal joint secondary to positive ulnar variance (Culp, 2005; Viegas and Ballantyne, 1987). The primary pathology in these cases is not limited only to the TFCC itself but also to the sequelae of chronic ulnar impaction between the ulna and the carpus, with secondary damage to surrounding structures including the lunotriquetral ligament, articular surfaces of the lunate, triquetrum and distal ulna (Culp, 2005; Palmer, 1989). When performing an arthroscopic debridement, the TFCC, adjacent synovitis and chondral changes are all debrided. It is essential to preserve the peripheral 2mm of the TFCC to maintain DRUJ stability.

If there is a positive ulnar variance, shortening of the ulna with either a diaphyseal ulnar shortening or arthroscopic wafer procedure should be performed. The arthroscopic wafer procedure involves resection of the prominent distal ulna through the TFCC tear (Darrow et al., 1985; Osterman, 1990; Verheyden and Short, 2001). Resection is continued until 2-3mm of ulna is removed over the radial two-thirds of the ulna to achieve a 1.5mm ulnar negative variance. Wnorowski et al recommended a wafer procedure be to the level of the subchondral bone, as this will unload the head of the ulna (Wnorowski et al., 1992). The forearm is rotated from pronation to supination to visualize and resect the full circumference of the ulnar head. Adequate resection is confirmed with fluoroscopy. Osterman reported pain relief in 73% and improvement in another 12% with this procedure (Osterman, 1990). These results are similar to the 78% good results reported for ulnar shortening by Darrow (Darrow et al., 1985; Osterman, 1990). The results of arthroscopic debridement of type 2 degenerative lesions have yielded good to excellent results in 75% of cases, with up to 5 years follow-up (Nagle, 1994).

Feldon et al stated that the wafer procedure is contraindicated if there is carpal instability or degenerative arthritis of the distal radioulnar joint (Feldon et al., 1992). Palmer and co-workers believe that this procedure is contraindicated if there is an associated lunotriquetral

tear, because it unloads the ulnocarpal joint and increases the carpal instability (Feldon et al., 1992). If instability is present, an open ulnar shortening osteotomy to prevent the ulnar impaction and tighten the ulnar carpal ligaments is often preferred. A lunotriquetral fusion may be required in some patients if there is gross lunotriquetral instability.

Deep sided tears of the TFC are uncommon, and can be difficult to diagnose. Arthroscopy of the DRUJ may be required to secure the diagnosis. The tear can then be debrided fro within the DRUJ (Video 2.1).

Video 2.1 – Arthroscopy of a patient with a partial deep tear of the TFCC. Note the superficial surface of the TFC, which provides a suspicion of the diagnosis. This was managed an arthroscopic debridement of the deep surface of the TFC within the DRUJ.

2.3.11 Ulnar stylo-carpal impaction

Stylo-carpal impaction is an uncommon cause of ulnar-sided wrist pain that is due to a long ulnar styloid that impinges on the carpus. It usually impinges onto the triquetrum, with wrist extension and supination. Typically, patients are reported to have an ulnar styloid which is longer than the average of 3-6mm (Biyani et al., 1990).

Confirmation of diagnosis of ulnar styloid carpal impingement has been based on provocation by placing the wrist into ulnar deviation and supination**,** and long ulnar styloid identified on plain radiographs.

Previous authors have described open excision of the ulnar styloid (Tomaino et al., 2001; Topper et al., 1997). This involves an open capsulotomy and osteotomy of the ulnar styloid near its base. The styloid is filleted from the TFCC. Unfortunately with this open technique, there is often a slow rehabilitation and persistent restricted range of motion. This was also the experience of the author. There have been no previous reports of arthroscopic management of ulnar stylo-carpal impaction. The aim of the study on ulnar stylo-carpal impaction was to develop a safe and efficient technique of arthroscopic management of ulnar stylo-carpal impaction.

2.3.12 Carpal instability

Radiological methods for assessing carpal instability include plain radiographs, fluoroscopy, arthrography, CT and MRI. Three-compartment arthrography will identify perforations of the intercarpal ligaments, but it does not provide accurate localization of the tears or the extent of the instability (Chung et al., 1996). Arthroscopy has been shown to be more sensitive than MRI in diagnosing intercarpal ligament and TFCC injuries (Morley et al., 2001).

Arthroscopy is now considered the gold standard for diagnosing carpal instability. It has the advantage of direct visualisation of the scapho-lunate and lunotriquetral ligaments (Cooney et al., 1990; Ruch and Bowling, 1998). The state of the ligament, the extent of the ligament injury and whether there is a repairable ligament stump, can all be assessed. Associated haemorrhage, synovitis, chondral damage and degenerative changes (e.g. radial styloid degenerative osteoarthritis) can also be visualized.

When performing infiltration into the mid-carpal joint, a leakage of saline through the radiocarpal portals indicates that there must be a tear of the lunotriquetral ligament or scapho-lunate ligament (Video 2.2). This is the same concept as that seen with an arthrogram where the mid-carpal joint is injected and a leakage of contrast is seen in the radiocarpal joint on follow-up radiographs (Chung et al., 1996; Dennison and Weiss, 1999; Theumann et al., 2001).

Video 2.2 – Infiltration of the mid-carpal joint with saline. Leakage of the saline from the 6R portal is due to leakage of the intracarpal ligaments (scapho-lunate or lunotriquetral ligaments).

A tear of the scapho-lunate or lunotriquetral ligament can be seen in the radiocarpal joint. From the mid-carpal joint the degree of laxity between the scapho-lunate interval can be assessed. Geissler described a classification for assessment of scapho-lunate instability (see Table 2.4) (Geissler et al., 1996). This relies upon identifying whether an arthroscopic probe can be placed into the scapho-lunate interval, whether it can be rotated, or whether a 2.7 arthroscope can be advanced between the scapho-lunate interval. In addition, the presence of a step between the scaphoid and the lunate can also be assessed.

Table 2.4 - Geissler Arthroscopic Classification of Carpal Instability.

Grade	Description
I	Attenuation/haemorrhage of interosseous ligament as seen from the radiocarpal joint. No in congruency of carpal alignment in the mid-carpal space.
II	Attenuation/haemorrhage of interosseous ligament as seen from the radiocarpal joint. In congruency/step-off as seen from the mid-carpal space. A slight gap (less than width of a probe) between the carpal bones may be present.
III	In congruency/step-off of carpal alignment is seen in the radiocarpal and mid-carpal space. The probe may be passed through the gap between the carpal bones.
IV	In congruency/step-off of carpal alignment is seen in the radiocarpal and mid-carpal space. Gross instability with manipulation is noted. A 2.7mm arthroscope may be passed through the gap between the carpal bones (so-called “drive-through lesion”).

From - Geissler, 2005.

Under the same anaesthetic a fluoroscopic assessment of the wrist can be performed (Ruch and Bowling, 1998). If this is performed before draping then the opposite wrist can be used for comparison. This examination should include placing the wrist in a neutral position, moving to full ulnar deviation, applying an axial load and also applying traction across the wrist to see if there is abnormal distal translation of the scaphoid.

The Watson scapho-lunate instability test can be performed under fluoroscopy and/or arthroscopic vision (Cooney et al., 1990; Watson et al., 1988). Abnormal widening of the scapho-lunate interval and subluxation or dislocation of the scaphoid over the dorsal rim of the distal radius can be identified.

Scapho-lunate ligament injuries are relatively common and remain a clinical dilemma. Treatment options have varied from immobilisation, repair and reconstruction to salvage procedure (multiple references).

Whipple reported 80% good results at four years for arthroscopic reduction and percutaneous fixation of scapho-lunate and lunotriquetral tears (Whipple, 1995). Results were superior for those patients who underwent repair less than three months after injury if the scapho-lunate interval was less than 3mm. Assad reported poorer results, with persistent diastasis in a similar patient population using an arthroscopic assisted reduction and K-wire fixation (Assad et al., 1997).

A lunotriquetral injury may occur following forced ulnar deviation or pronation of the wrist or as part of a healed perilunate injury (Mayfield et al., 1980). Clinical assessment may identify localized tenderness, pain and instability with triquetrolunate ballottement (Reagan et al., 1984).

Lunotriquetral instability can also be assessed using the same arthroscopic assessment techniques and specific provocation tests (Bednar and Osterman, 1993). Pressure is placed directly onto the pisiform and on the dorsal aspect of the lunate. By squeezing the lunate volarly and the triquetrum dorsally, lunotriquetral instability is identified. The wrist is taken through radial and ulnar deviation with direct visualization of the lunotriquetral articulation.

2.3.13 Distal radius fractures

In 1814 Abraham Colles stated, “that the limb will at some remote period again enjoy perfect freedom in all its motions and be completely exempt from pain” (Colles, 1814). Unfortunately this has not been demonstrated to be true, with most studies reporting pain following management of distal radius fractures. However it remains a plausible goal!

Knirk and Jupiter reported that radiological arthritis developed in 91% of those wrists that had any degree of articular step, and in all of those with a step greater than 2mm (Knirk and Jupiter, 1986). Other authors have confirmed this in the ensuing years (Bassett, 1987; Bradway et al., 1989; Melone, 1986; Missakian et al., 1992).Melone stated that articular fragment separation of as little as 2mm is prone to persistent and progressive joint incongruity with a high probability of development of degenerative arthritis (Melone, 1993).

Failure to reduce intra-articular fractures of the distal radius predisposes to pain, restricted range of motion and degenerative arthritis (Bradway et al., 1989; Knirk and Jupiter, 1986. Malposition in these injuries relates not only to parameters such as radial height, radial angle and volar tilt but also to the accuracy of intra-articular reduction (Melone, 1986; Missakian et al., 1992; Pogue et al., 1990).

A number of authors have recommended open reduction and internal fixation of comminuted intra-articular fractures of the distal radius. However, this can be a difficult undertaking and a dorsal and volar approach may be required (Pogue et al., 1990; Wolfe et al., 1995). Exposure of the fracture strips the soft tissues and causes devascularisation of the bone fragments. To provide adequate exposure of the articular surface requires further capsular and ligamentous dissection, which causes additional soft tissue injury and may lead to post operative stiffness or radiocarpal instability (Axelrod et al., 1988; Bradway et al., 1989; Culp and Osterman, 1995; Levy and Glickel, 1993; Wolfe et al., 1995). Because of these problems, some surgeons have advocated limited open reduction techniques that utilise selective surgical exposure of displaced articular fragments (Axelrod et al., 1988; Bradway et al., 1989; Fernandez and Geissler, 1991). With these techniques, complete visualisation of the articular surface is difficult.

Many authors have reported the use of wrist arthroscopy in the management of intra-articular distal radial fractures (Cooney et al., 1980; Culp and Osterman, 1995; Geissler, 1995; Geissler, 1997; Hanker, 1996; Levy and Glickel, 1993; Roth et al., 1995; Wolfe et al., 1995).

It is less invasive and allows a magnified view of the articular surface as well as assessment of triangular fibrocartilage, scapho-lunate and lunotriquetral ligaments. All of the arthroscopic reports have noted a high incidence of associated ligament injuries.

Culp and Osterman reported on 27 cases treated with arthroscopically assisted reduction of intra-articular distal radial fractures (Culp and Osterman, 1995). They reported 10 excellent and 12 good results using the Gartland and Werley classification (Gartland and Werley, 1951). Pain, satisfaction and complications were not reported. Wolfe et al reported that six of their seven patients had an excellent result using the Gartland and Werley (G&W) score but did not mention whether any concomitant intracarpal injuries were present (Wolfe et al., 1995). Hanker reported on 27 cases and stated that it improved outcome in complex intra-articular distal radial fractures, but he did not report any objective results (Hanker, 1996). Other authors have also reported on arthroscopically assisted reduction of distal radius fractures but did not report objective results (Geissler, 1995; Levy and Glickel, 1993).

In view of the deficiencies identified in the literature, the author decided to perform a comprehensive review of the outcome of patients managed with an arthroscopic assisted reduction of distal radius fractures. The aim is to develop a safe and efficient therapeutic technique of wrist arthroscopy for the management of distal radius fractures. To aim at an anatomical reduction of the articular surface using minimally invasive techniques.

When performing arthroscopy for distal radial fractures, the risk of compartment syndrome is a concern. However, few cases of compartment syndrome following arthroscopy have actually been reported (Nillium and Rosser, 1983; Peek and Haynes, 1984). Cases have been reported following knee arthroscopy. Safety measures to minimize fluid extravasation include the use of gravity-fed systems, wrapping the forearm with an elastic bandage and using large portals to allow free egress of fluid (Peek and Haynes, 1984). Irrigation pumps are likely to increase fluid extravasation. If surgery is delayed for 48 hours following a distal radial fracture, the fracture haematoma will have clotted, minimising intra-articular bleeding and fluid extravasation. Simple elevation of the arm and cessation of arthroscopy will relieve the problem of fluid extravasation (Darrow et al., 1985).

Since performing the author's arthroscopic study of distal radius fractures, fixed angle plates have been introduced and become popular (8415) (Orbay and Fernandez, 2002; Orbay and Fernandez, 2004).

2.3.14 Scaphoid fractures

Percutaneous fixation techniques have become increasingly popular for management of scaphoid fractures (Inoue and Shionoya, 1997; Wozasek and Moser, 1991). The concept of using wrist arthroscopy to assist in scaphoid fractures was introduced by Terry Whipple and subsequently reported by others (Geissler and Hammit, 2001; Slade et al., 2003; Whipple, 1995). It is indicated for displaced but reducible scaphoid fractures and undisplaced but unstable fractures (Geissler and Hammit, 2001). The magnification provided by arthroscopy allows accurate assessment of fracture reduction. In addition, arthroscopy allows assessment of the other injuries within the carpus, including injuries to the interosseous ligaments, triangular fibrocartilage and osteochondral fractures (Shih et al., 2005).

Arthroscopy is valuable in ensuring that there is correct rotation of the fracture. The author has seen a number of scaphoid fractures that were considered to be simple and stable but, when assessed arthroscopically, have been surprised at the malrotation, instability and associated chondral injuries.

Jigs can be utilized to stabilize the fracture and provide compression across the fracture prior to fixation (Geissler and Hammit, 2001; Slade et al., 2003; Whipple, 1995). A K-wire can be positioned with accuracy and a cannulated screw inserted over the top. The other end of the jig is introduced through a 1-2 portal and positioned directly adjacent to the scapho-lunate ligament. Compression of the jig will stabilise the scaphoid. However, it is critical to ensure that reduction is obtained as the jig may displace the fracture.

Fractures of the proximal pole of the scaphoid can also be managed with dorsal percutaneous fixation (Slade et al., 2003). A double cut K-wire is advanced through the proximal pole of the scaphoid into the centre of the circle identified on the fluoroscopy unit. It is advanced through the wrist to pierce the skin on the radial volar aspect of the thumb. This wire will likely be within the trapezium. The wire is withdrawn from the volar aspect so that the wrist can be extended. The position of the fracture and wire can now be better assessed with fluoroscopy and placed in the standard set-up for wrist arthroscopy. Once correct wire position is confirmed, the wire is advanced from volar to dorsal. Over this wire a cannulated headless screw is inserted into the scaphoid from the dorsal aspect.

Wrist arthroscopy is also of use in a proportion of scaphoid non-unions. Slade et al reported the use of arthroscopy in the assessment and management of selected scaphoid fibrous non-

unions (Slade et al., 2003). CT scan showed well-aligned fractures with minimal sclerosis (<1mm) and no cyst formation. Arthroscopy was used to confirm reduction and the presence of an intact cartilaginous envelope. The fracture was seen as a dark line on the articular cartilage and probing revealed firm fibrous union. These authors recommended percutaneous compression screw fixation without bone grafting and had 100% union at 14 weeks in this group of patients.

Arthroscopic excision of the proximal pole of the scaphoid for Preisser's disease has been reported (Menth-Chiari and Poehling, 2000). Ruch et al reported an arthroscopic radial styloidectomy and distal scaphoid excision for avascular necrosis of the proximal pole of scaphoid with non-union (Ruch et al., 1998). There was improved pain and motion despite increased carpal collapse in these three patients.

2.3.15 Synovectomy

Synovectomy has historically been the first-line surgical treatment of joints affected by rheumatoid arthritis for which medical management has failed. Synovectomy for rheumatoid arthritis appears to slow down and in some cases halt the progression of the disease (Smiley and Wasilewski, 1990; Taylor, 1979). Experience with other joints has shown that synovectomy should be performed during the early stages of the disease, before severe joint destruction develops. The concerns with open synovectomy are the prolonged rehabilitation and the possibility of loss of motion.

Arthroscopy provides a magnified view of the pathologic synovium, which typically accumulates on the volar ligaments of the radiocarpal joint (Adolfsson and Nylander, 1993; Richards and Roth, 1991). A complete synovectomy can be performed by alternating the resector between the multiple portals.

A mid-carpal synovectomy is also performed although it is commonly spared in rheumatoid arthritis (Adolfsson and Nylander, 1993). Adolfsson and Nylander reported the results of arthroscopic synovectomy in 16 patients (18 wrists) with rheumatoid arthritis. All patients experienced a reduction in pain at rest, during activity and at night. The average arc of extension and flexion improved from 69° to 90°and no patient experienced a decrease in the range of motion. The average grip strength improved 87% after 6 months. There were no complications in this series (Adolfsson and Nylander, 1993).

Arthroscopic synovectomy of the wrist is now an established procedure that offers superior visualization, easy access and effective removal of the pathologic synovium in an outpatient setting (Adolfsson and Nylander, 1993; Roth, 1988).

2.3.16 Kienböcks disease

In 1910 Robert Kienböck described avascular necrosis of the lunate based on plain radiographs. Kienböck's disease is idiopathic avascular necrosis of the lunate which is more common in males and typically presents between the ages of 20 and 40 years. Patients often present with wrist pain, swelling, restricted range of motion and difficulty performing activities of daily living.

The ulnar variance of the wrist is considered to be an important etiological factor in the development of Kienböck's disease (Gelberman et al., 1975). It is considered that a negative ulnar variance leads to increased joint loading that affects vascularity of the lunate (Gelberman et al., 1983). Patients with a negative ulnar variance are often recommended to have a joint levelling procedure (Amadio and Wolfe, 2005).

Lichtman's radiological classification of Kienböck's disease is commonly used to grade the condition (Lichtman et al., 1977). However, inter-observer variability studies have shown a poor reliability (Goldfarb et al., 2003; Hjorth Jensen et al., 1996; Jafarnia et al., 2000).

The management of Kienböcks disease has been very controversial (Amadio and Wolfe, 2005). Non-operative management has included immobilisation (Stahl and Reis, 1986). The results of non-operative treatment have varied, but have included a progression of the disease process with further collapse of the lunate (Mikkelsen and Gelineck, 1987). For those patients who fail to improve with non-operative modalities, surgical treatment is often offered.

The number of surgical procedures described is of concern. Lunate excision has been reported, but may produce a severe carpal instability and a disabled wrist (Kawai et al., 1988). Replacement arthroplasties have been reported using silicone, titanium and cement (Alexander et al., 1990; Alexander et al., 1990; Carroll, 1983; Hastings et al., 1983; Ishiguro, 1984). However, lunate replacement procedures will not prevent further collapse of the carpus (Amadio and Wolfe, 2005).

Of the operative techniques, joint leveling procedures have been the most popular, especially in patients who have a negative ulnar variance (Frykman et al., 1988; Gelberman et al., 1975;

Nakamura et al., 1993). Examples include radial shortening (Almquist and Burns, 1982), ulna lengthening (Amadio and Wolfe, 2005) and angular osteotomy of the radius (Nakamura et al., 1993). Capitate shortening also changes the joint loading at the radiolunate articulation, but from the mid-carpal joint perspective (Almquist, 1987).

Limited wrist fusions in the form of an STT arthrodesis have previously been popular (Allieu et al., 1991; Watson, 1980; Watson et al., 1996). The STT fusion had the advantage of maintaining carpal height and unloading the radiolunate articulation. Miniami reported that there was a progression of the radioscaphoid degeneration following STT arthrodesis (Minami et al., 1994). Other limited wrist fusions in the form of radio-scapho-lunate and capito-hamate fusion have also been reported (Chuinard and Zeman, 1980). Proximal row carpectomy has also been utilised (Begley and Engber, 1994).

Revascularisation procedures address the primary problem of inadequate blood supply (Botte et al., 2004; Leblebicioglu et al., 2003). Moran reported a series of 48 cases in which post-operative MRI showed revascularisation in 60% of cases (Hori et al., 1979). Those patients with improved vascularisation had significantly improved pain scores. Moran recommends an external fixateur or pinning the scaphocapitate joint to unload the joint for a period 8-12 weeks. However, revascularisation procedures are only likely to be effective in those patients who have not yet had any carpal collapse.

The use of wrist arthroscopy for the treatment of Kienböck's disease has recently been reported by Menth-Chiari et al (Menth-Chiari et al., 1999.). They utilised arthroscopy for both assessing the diseased joints and debriding the necrotic lunate. All patients in their study were graded as Lichtman IIIA or IIIB and all experienced relief of their painful mechanical symptoms. All patients were treated with debridement regardless of the arthroscopic findings. It was concluded that although the progression of the disease cannot be altered, arthroscopic assessment and debridement offers a benefit in clinical outcome and may defer more definitive surgery (Menth-Chiari et al., 1999).

However in the more advanced cases and in the higher demand patients, this technique does not provide a functional articular surface. The details of articular changes and their distribution were unknown. For those patients who fail to recover or have a relapse of pain, a recommendation for the secondary procedure had not been determined.

The role of arthroscopy in the diagnosis of Kienböck's disease was unknown. It was this deficiency that led to the study to assess the role of arthroscopy in Kienböck's disease, to document the articular changes of Kienböck's disease and to consider the development of a classification system to direct the secondary procedure, if that were required.

2.3.17 Ganglion

Ganglions have historically been managed with open excision, although there has been concern about slow rehabilitation and wrist contracture in some patients (Wright et al., 1994; Young et al., 1988). The goal of arthroscopic ganglion resection is to reduce scarring and avoid capsular stiffness that may be associated with an open ganglion excision (Osterman and Raphael, 1995).

In addition, any underlying instability of the intrinsic scapho-lunate ligament can be thoroughly assessed at the time of arthroscopy (Culp, 2005; Watson et al., 1989). The ganglion and the adjacent synovitis can be visualized on the scapho-lunate ligament and the adjacent dorsal capsule (Viegas, 1986; Whipple, 1992).

Osterman and Raphael reported excision of the dorsal ganglion using standard wrist arthroscopy portal sites (Osterman and Raphael, 1995) . The scope is placed in the 6-R portal and the instruments is the 1-2 portal. The ganglion is resected from the dorsum of the scapho-lunate ligament. Osterman reports approximately two-thirds of patients will have a visible pearl-like ganglion stalk. When such a stalk is not seen, the origin is assumed to be from the dorsal capsule, in which case synovitis is usually noted. A needle placed through the skin and extended into the stalk is utilised. A ganglion portal (almost always equivalent to the standard 3-4 portal) can also be established to assist with excision of the ganglion. A full-radius resector or basket punch is used to resect a 1cm diameter of dorsal capsule at the ganglion origin. Care should be taken to avoid injury to the scapho-lunate ligament and extensor tendons. Dorsal synovitis, where present, is debrided. In one-third of cases, the underlying extensor tendons may be visible. The wrist is removed from the traction tower and re-examined. It is important to ensure that the extra-articular portion of the ganglion has been fully ruptured. Osterman reported only one recurrence in his series of 150 patients.

Ho reported on excision of the volar wrist ganglion by placing the resector into the interligamentous sulcus located between the RSC and LRL ligaments. The resector is advanced through this interval to resect the ganglion tissue (Ho, 2007). Ho cautioned that the volar ganglions from the STT joint are at the distal wrist crease and currently can not be removed with arthroscopic techniques.

2.3.18 Intra-osseous ganglion of the lunate

Intra-osseous ganglions have been reported most frequently in the lower limb, principally around the hip, knee and ankle (Schajowicz et al., 1979). These lesions are typically found in the epiphyses of long bones, with the two most common locations being the femoral head and the medial malleolus. Less than a fifth of cases reported are found in the carpal bones, where the ganglion may be an infrequent cause of chronic wrist pain. The pathogenesis remains obscure (Tham and Ireland, 1992; Waizenegger, 1993). Bone scans and computed tomography (CT) scans are used to distinguish these radiolucent carpal lesions from other pathologies, in particular degenerative cysts and osteoid osteomas (Tham and Ireland, 1992). Magnetic resonance imaging shows the bony extent of the lesion and additionally may help to delineate the presence of an extraosseous extension of the ganglion (Sullivan and Berquist, 1991).

(Tham and Ireland, 1992; Waizenegger, 1993) Theories of pathogenesis include synovial herniation, neoplasia, metaplasia of mesenchymal precursor cells, proliferation of synovial rest cells and traumatic mucoid degeneration of connective tissue (Tham and Ireland, 1992; Waizenegger, 1993). The shear stresses concentrated at the scapho-lunate ligament insertion may predispose some individuals to develop the precursor cells that form the intra-osseous ganglion (Young et al., 1988)**.**

Intra-osseous ganglions are pathologically identical to the soft tissue variety, with a thin wall of compressed collagen and fibroblasts containing a clear viscous fluid that has a high concentration of hyaluronic acid (Green and O'Brien, 1978; Kambolis et al., 1973; Mogan et al., 1981; Sullivan and Berquist, 1991; Tham et al., 1999; Tham and Ireland, 1992; Waizenegger, 1993; Young et al., 1988). There is no endothelial or synovial lining. A thin sclerotic margin of bone often surrounds the defect within the lunate (Waizenegger, 1993). Bone scans invariably show increased uptake localized specifically within the involved carpal bone, perhaps because of this repair response or from a micro fracture in the thin sclerotic margin.

Symptoms appear to correlate uniformly with having positive results from a bone scan (Waizenegger, 1993). Persistence and severity of symptoms rather than radiologic findings determine the need for further treatment (Mogan et al., 1981). If symptoms interfere with function at work or during recreation, then surgery is indicated (Tham and Ireland, 1992; Waizenegger, 1993).

Open curettage and bone grafting has been performed for patients with constant symptoms who have severely restricted occupational or recreational activities (Kambolis et al., 1973; Mogan et al., 1981; Sullivan and Berquist, 1991; Tham and Ireland, 1992; Waizenegger, 1993). Relief of symptoms, with curettage and grafting procedures was not uniform or predictable (Schajowicz et al., 1979; Tham and Ireland, 1992; Waizenegger, 1993). Tham and Ireland treated 9 patients with 1 poor and 2 fair results owing to pain (Tham and Ireland, 1992). The poorer results were noted for lesions that appeared to extend to the scapho-lunate region. Waizenegger reported incomplete pain relief for 6 patients, which affected their performance at work (Waizenegger, 1993).

Despite bone graft and curettage, the site of the lesion can still be identified on follow-up radiographs (Kambolis et al., 1973; Mogan et al., 1981; Sullivan and Berquist, 1991; Tham and Ireland, 1992; Waizenegger, 1993), the sclerotic margin still being clearly evident although the lesion becomes replaced with trabeculated bone.

There have been no reports in the literature of arthroscopic management of intra-osseous ganglion of the lunate. The aim is to develop a safe and effective therapeutic wrist arthroscopy technique for the management of intra-osseous ganglion of the lunate.

2.3.19 Scapho-trapezio-trapezoid arthritis

Scapho-trapezio-trapezoid (STT) joint arthritis is a common clinical condition. Assessment of cadaveric wrists has demonstrated that degenerative changes are seen in 39% of specimens (Moritomo et al., 2000). Moritomo et al have noted that the most common site of degenerative change is on the ulnar side of the distal scaphoid and centrally on the trapezoid and trapezium(Moritomo et al., 2000).

Involvement of the STT joint occurs in 15% to 30% of wrists and is the second most common pattern observed (Rogers and Watson, 1990). Concomitant trapeziometacarpal arthritis occurs in the majority of patients, but isolated pathology occurs in 2% to 16% of the population

(Chamay and Piaget-Morerod, 1994; Garcia-Elias et al., 1999). It is more common in postmenopausal women (Armstrong et al., 1994). Symptomatically isolated STT disease leads to tenderness over the palmar aspect of the thenar eminence and is an important differential diagnosis in radial wrist pain. Flexor carpi radialis tendinitis and radiopalmar ganglions can be associated with STT joint arthritis (Srinivasan and Matthews, 1996).

Previous surgical treatments reported after failed conservative treatment include STT joint fusion (Srinivasan and Matthews, 1996), excisional arthroplasty with (Eiken, 1979) or without (Garcia-Elias et al., 1999) a silicone spacer. Pain relief is not uniform in these series, with post-operative morbidity from complications being noted. STT arthrodesis has a high reported complication rate, which includes painful non-union, radioscaphoid impingement and hardware complications (Garcia-Elias et al., 1999; Ishida and Tsai, 1993; Srinivasan and Matthews, 1996). Secondary arthritis of radioscaphoid or trapeziometacarpal joints can also occur. Excision arthroplasty of the distal scaphoid will leave almost 40% of patients with mild pain. Excision of the distal scaphoid resulted in a change in the carpal alignment with a DISI pattern in 12 of 21 cases (Garcia-Elias et al., 1999). It was the author's experience that following an excision arthroplasty that the patients developed a gross DISI deformity, which was associated with pain and disability. For this reason the author abandoned the excision arthroplasty technique.

With wrist arthroscopy the articular changes can be visualised and a debridement performed. Arthroscopic debridement has been used to treat degenerative arthritis in the knee for many years in many centres (Bert and Maschka, 1989; Dandy, 1991). It is considered a temporising treatment in patients who were felt to be too young for total knee replacement. Arthroscopic debridement has proven to be an effective method of achieving pain relief in the knee in two-thirds of patients for 2 to 5 years with a low morbidity (Bert and Maschka, 1989; Dandy, 1991). Considerable pain relief was noted in one-third of patients lasting into the medium term. Arthroscopic procedures allow further assessment of the remainder of the joint as well as other therapeutic interventions.

There has not been a clinical series of degenerative STT joint arthritis managed arthroscopically in the literature. The aim of the STT paper was to develop and report a safe and effective therapeutic method of arthroscopic management of STT joint arthritis.

2.3.20 Chondral defects

Chondral defects are reported to be not an infrequent cause of occult wrist pain (Poehling and Roth, 1991; Whipple, 1992). Clinical diagnosis of chondral defects is difficult because the patient often has only diffuse tenderness. Chondral defects are poorly diagnosed by standard imaging modalities, including MR imaging (Cerofolini et al., 1990). If wrist pain persists despite conservative measures, then wrist arthroscopy may be considered.

Partial-thickness cartilage lesions have some potential to heal, but full-thickness cartilage defects have no such potential (Poehling and Roth, 1991). The fate of particular cartilage adjacent to a defect depends on the strength of its edges and the mechanical stability of the joint (Poehling and Roth, 1991). If the subchondral bone is disrupted, granulation tissue is formed which is transformed into fibrocartilage (Johnson, 1986). The clinical application of this phenomenon is abrasion and drill chondroplasty. Unfortunately, the fibrocartilage produced becomes soft and is poorly resistant to wear (Johnson, 1986).

At arthroscopy, the size and stability of the chondral defects can be assessed. Chondral lesions are smoothed to reduce mechanical symptoms and to minimise the production of intra-articular debris that would facilitate the degenerative process. Whipple advises that patients often have symptomatic relief following abrasion arthroplasty for lesions in the wrist less than 5mm in diameter (Whipple, 1992). Abrasive arthroplasty is unlikely to be successful if extensive changes are present; however, the lavage of debris and lysomal enzymes from the joint will provide temporary relief of symptoms in some patients (Poehling and Roth, 1991).

Poehling and Roth reported a multicentre study of chondral defects in the wrist diagnosed with arthroscopy (Poehling and Roth, 1991). Cartilage lesions were classified as primary if the source of symptoms was judged to be the articular cartilage and secondary if it was from another cause (e.g., ligament instability or fracture). Eighty-three per cent of patients with primary lesions improved, but only 55% with secondary lesions (Poehling and Roth, 1991).

Arthroscopic debridement of chondral lesions in the wrist has been described in a number of anatomical sites. This includes the STT joint, radiocarpal joint in Kienböck's disease and the proximal pole of the scaphoid (Ashwood et al., 2003; Menth-Chiari and Poehling, 2000; Ruch et al., 1998). Post-traumatic chondral lesions are not uncommon following wrist injuries, including distal radius fractures. Patients who are most likely to obtain a good result with arthroscopic debridement are those with mechanical symptoms.

Patients with a type 2 lunate are at increased risk of developing degenerative osteoarthritis at the proximal condyle of the hamate (Viegas et al., 1990). This is a less common cause of ulnar-sided wrist pain. The proximal condyle of the hamate can be debrided arthroscopically through a mid-carpal ulna portal (Thurston and Stanley, 1999).

2.3.21 Wrist joint contracture

Following trauma or surgery to the wrist, stiffness of the wrist is common. The etiology of contracture of a joint can be classified into either intra-articular or extra-articular (Cooney, 1993). Intra-articular and capsular injuries and prolonged immobilization will stimulate arthrofibrosis (Cooney, 1993).

All patients undergoing treatment for contracture of the wrist joint should be given a full trial of non-operative treatment including physiotherapy and splinting. Surgical treatment has been successfully used for contracture of the knee, shoulder and elbow (Jones and Savoie, 1993; Kleinman and Graham, 1996; Morrey, 1992; Richmond and al Assal, 1991; Warner et al., 1996; Warner et al., 1997; Watson, 1988; Zanotti and Kuhn, 1997).

Arthroscopic management of arthrofibrosis of the knee was described by Richmond Assam (Richmond and al Assal, 1991). Arthroscopic capsular release of the knee, shoulder and elbow has been reported to provide an improved range of motion with little operative morbidity (Jones and Savoie, 1993; Richmond and al Assal, 1991; Warner et al., 1996; Warner et al., 1997). Cadaveric studies have been performed to assess the proximity of major neurovascular structures and the safety of arthroscopic capsulotomy in the shoulder (Zanotti and Kuhn, 1997).

Watson and Turkeltaub described an open surgical release for a radiocarpal joint contracture using both a volar and dorsal surgical approach (Watson, 1988). Open capsulectomy of the distal radioulnar joint has also been described for post-traumatic contracture of the distal radioulnar joint capsule (Kleinman and Graham, 1996).

The aim is to develop a safe and efficient therapeutic technique of wrist arthroscopy for the management of wrist contracture. To determine the proximity of the major neurovascular structures on the volar capsule of the wrist.

2.3.22 Resection arthroplasty

Many procedures that were previously performed through an arthrotomy can now be performed arthroscopically, with the advantages of decreased post-operative pain and less stiffness.

Arthroscopy also allows accurate assessment of the articular surfaces of the capitate and the lunate fossa prior to proceeding with a proximal row carpectomy. In addition a proximal row carpectomy can be performed as an arthroscopic procedure (Culp et al., 1993; Roth and Poehling, 1990). Intra-operative radiographs were used to confirm the desired bony resection.

Arthroscopic hemiresection of the distal ulna has also been performed (Roth and Poehling, 1990). The forearm is rotated to ensure an adequate ulnar head resection. Intra-operative radiographs are important to ensure that an adequate amount of bone has been resected.

Other arthroscopic procedures that have been reported are radial styloidectomy and excision of the proximal pole of the scaphoid for a scaphoid non-union (Whipple, 1988). Resection of the lunate for Kienböck's disease could also be performed arthroscopically,

2.3.23 Chronic wrist pain

Chronic wrist pain can be considered mechanical or dystrophic (Darrow et al., 1985). Patients with mechanical symptoms such as catching, clicking, locking and pain that increases with activity and decreases with rest, are more likely to have a good result following wrist arthroscopy (Darrow et al., 1985). In contrast, patients with dystrophic symptoms, such as burning pain that is often worse at night, exacerbated by minimal activity or associated with cold insensitivity, dysesthesia, paresthesia or vasomotor changes, are less likely to obtain symptomatic relief following arthroscopy (Darrow et al., 1985).

2.3.24 Complications

Complications of wrist arthroscopy are uncommon with authors reporting rates of approximately 2% (Chen, 1979) (Culp, 1999; Warhold and Ruth, 1995). Most complications are related to the size of the instrumentation within a small joint space. Care must be taken with creation of portal sites as injury to the extensor tendons, radial artery and branches of the radial and ulnar nerve have all been reported. EPL is the tendon most at risk during wrist arthroscopy with creation of the 3-4 portal. Other reported complications include infections,

reflex sympathetic dystrophy, and those relating to implanted material such as sutures or Kirschner wires (Culp, 1999; De Smet, 2002; del Pinal et al., 1999). Skin lacerations on finger traps have been reported and the use of flexible nylon finger traps has been advocated in those patients with very friable skin (e.g. rheumatoid arthritis).

The radial artery is at risk during the establishment of the 1-2 portal. To prevent injury to the radial artery, the portal should be just volar to the extensor pollicis longus tendon. The superficial branch of the radial nerve and the dorsal cutaneous branch of the ulnar nerve are at risk when establishing the 1-2 and 6U portals respectively (Pianka, 1992). Using mini-open incisions and dissecting the soft tissue minimises these complications, particularly on the radial and ulnar aspects of the wrist.

2.4 Knowledge deficiencies

2.4.1 Anatomy

2.4.1.1 Scaphoid kinematics

Association between the scaphoid kinematics and morphology of the mid-carpal joint is unknown.

There is no known simple radiological marker of scaphoid kinematics.

2.4.1.2 Triquetro-hamate joint

The literature is confusing on the morphology of the triquetro-hamate joint. The morphological types of triquetro-hamate joint have not been described.

The association between the configuration of the triquetro-hamate joint and the lunate type is unknown.

The association between the morphological types of triquetro-hamate joint and kinematics of this joint have not been determined.

2.4.2 Imaging

2.4.2.1 Longitudinal computed tomography of the scaphoid

The previously reported techniques have incorporated immobilisation devices or have been preformed in ulnar deviation that can be uncomfortable for the patient. A standardised method of performing a CT scan that is comfortable and simple has not been developed.

There is no method to ensure that the correct longitudinal scanning plane has been obtained.

2.4.2.2 Assessment of humpback deformity of the scaphoid

The role of computed tomography scans in the assessment of scaphoid deformity has not been determined.

It is not known if the intrascaphoid angle method of assessment of the humpback deformity is reliable.

No inter-observer variability study of the assessment of the humpback deformity of the scaphoid has been performed.

2.4.2.3 Clinical utilisation of computed tomography.

The clinical role of computed tomography of the scaphoid has not been determined.

No method of templating of scaphoid fractures has been reported using computed tomography.

The difficulties in assessment of fracture union have not been defined.

2.4.2.4 Portable operative fluoroscopy

There have been no reports on the use of fluoroscopy in surgical management of disorders of the wrist or upper limb.

2.4.3 Arthroscopy

2.4.3.1 Kienböck's disease

a. There have been no published studies documenting the arthroscopic changes in Kienböck's disease.

b. No arthroscopic classification system has been developed for the assessment of articular changes in Kienböck's disease.

c. There are no recommendations available that provide guidance to treatment based on arthroscopic findings.

d. There has been no correlation performed between the arthroscopic and radiological findings.

e. The natural history of the articular findings is unknown.

2.4.3.2 Distal radius fractures

A number of studies on arthroscopic assisted reduction of distal radius fractures have been reported. However, most have either a small series or do not provide detailed subjective and objective follow-up.

The role of fluoroscopy in assessment of fracture reduction and fixation has not been defined.

There are no reported correlations of incidence of wrist pain compared to post operative radiological findings.

2.4.3.3 Wrist contracture

There are no reports of proximity of the volar wrist capsule to the major neurovascular structures.

There are no reports of arthroscopic release of the volar wrist capsule.

There are no reports of arthroscopic release of the dorsal wrist capsule.

2.4.3.4 Intra-osseous ganglion of the lunate

There are no reports of arthroscopic management of intra-osseous ganglion of the lunate.

2.4.3.5 STT arthritis

No peer review papers have been published on the role of arthroscopic debridement of the STT joint of the wrist.

There is limited information on the portals for arthroscopy of the STT joint.

There has been no comparison of cadaveric findings of STT joint arthritis to arthroscopic findings in symptomatic individuals.

2.4.3.6 Ulnar stylo-carpal impingement

Diagnosis of ulnar stylo-carpal impingement is based on clinical examination and plain radiographs. The role of fluoroscopy and 3D CT scans in the provocation position has not been determined.

Identification of the ulnar styloid by arthroscopy has not been reported.

There are no reported techniques of arthroscopic management of ulnar stylo-carpal impaction.

The role of fluoroscopy to assist in identification and excision of the ulnar styloid has not been determined.

2.5 Relationship of the literature to the experimental program.

2.5.1 Anatomy

The aims of the experimental program have been established to fill the knowledge deficiencies in the literature on scaphoid kinematics. This includes the comparison of the kinematics with the morphology of the mid-carpal joint. The previous published methods of assessment of scaphoid motion (Craigen and Stanley, 1995) were used and compared to the lunate morphology as previously published by Viegas (Viegas et al., 1993). The exact methodology of assessment of the scaphoid kinematics and the lunate type were the same as those previously published. Therefore the literature was the platform from which the study was developed.

The study on the triquetro-hamate joint was aimed at determining the morphology of the joint because of confusion in the literature as to the correct morphology. The discussion of the paper addressed the relationship of the findings to the previous literature.

2.5.2 Imaging

The aims of the experimental program have been established to fill the knowledge deficiencies in the literature, including the assessment of the humpback deformity, templating of the scaphoid to correction of the deformity and the utilisation of the fluoroscopy to assist in surgical procedures on the wrist.

The paper on the humpback deformity was established because of concerns about utilising the previously published techniques of assessment. The assessment of the humpback deformity was performed with direct comparison to the method previously published by Amadio (Amadio et al., 1989). The methods of assessing the inter-observer variability were those previously published (Shrout and Fleiss, 1979).

2.5.3 Arthroscopy

The aims of the experimental program have been established to fill the knowledge deficiencies in the literature, including the development of new diagnostic techniques for assessment of Kienböck's disease. The role of arthroscopy in the management of Kienböck's disease as a therapeutic tool had been explored but remained unknown as a diagnostic tool.

Development of new therapeutic techniques for the management of distal radius fracture, STT arthritis, intra-osseous ganglion of the lunate, wrist contracture, and ulnar stylo-carpal impingement.

The objectives chosen were also related to the deviancies in the literature. For example, it was critical to determine the proximity of the major neurovascular structures to the volar capsular of the wrist. For safety reasons this was performed on a cadaveric model.
Other objectives were related to established principles in the literature such as the choice of outcome measures, assessment of complications and comparison to historical controls published in the literature.

Research design

The design of the procedures will be based on techniques published in the literature. The open techniques published for management of wrist contracture, intra-osseous ganglion of the lunate, STT arthritis, ulnar stylo-carpal impingement and distal radius fractures were assessed to utilise the principles already established and to try and adapt them to arthroscopy.

There are situations where arthroscopic management has unique challenges, which are not readily apparent on initial review of the literature. For example, identification of the ulnar styloid at arthroscopy, obtaining a safe portal when performing STT joint arthroscopy and assuring safety when performing arthroscopic capsular release. Although the literature does provide these answers, the concepts learnt by reading the literature and trying to understand them help to predict the problems and solve them when they are encountered. This is particularly important with surgery.

Methodology

The indications for the arthroscopic procedures will be based on those already established in the literature for the open procedures.

The subjective, objective and radiological outcome measures chosen were based on those already in the literature.

The complications recorded are the some as those reported in open techniques. These include RSD, infection and neurovascular injuries following arthroscopy.

The determination of safety and efficiency will include comparing results to previously published works.

Chapter 3 - RESEARCH UNDERTAKEN - ANATOMY

3.1 Introduction

The research performed covers published papers on anatomy, imaging and arthroscopy. The papers in each section are individually discussed. The discussion of each paper will commence with the research aims and objectives of the individual study. It includes the principles of study methodology and the main findings of the published research. It is not a restating of the published paper.

This anatomy section provides a review of the research undertaken on the anatomy of the normal wrist. It includes two papers which are on scaphoid kinematics and morphology of the triquetro-hamate joint respectively.

3.2 Influence of lunate type on scaphoid kinematics

3.2.1 Research aims

The aim was to assess the effect of the lunate type on scaphoid kinematics.

3.2.2 Research objectives

To measure scaphoid translation and flexion using fluoroscopic assessment of the wrist in radial and ulnar deviation (Craigen and Stanley, 1995; Garcia-Elias et al., 1995).

To determine the lunate type, as described by Viegas, using fluoroscopic assessment.

To correlate the type of scaphoid motion to the type of lunate identified.

To determine the association between lunate type and scaphoid kinematics.

3.2.3 Research performed

One hundred healthy volunteers with asymptomatic wrists between ages 20-50 years were reviewed.

A standardized x-ray protocol was used and recorded on a proforma sheet. Posterior-anterior (PA) fluoroscopic radiographs were performed with the upper limb in a standardised position

(Hardy et al., 1987). The volunteer was asked to actively position the wrist in maximal radial deviation, neutral position and ulnar deviation sequentially, while leaving the palm of the hand in the fluoroscopic tube (Navarro, 1921). A metallic magnification marker was placed on the fluoroscan plate, at the level of the carpus on the ulnar side, to allow correction for any magnification.

Radiological parameters were measured with a Vernier electronic digital calliper. All measurements were performed independently on two separate occasions by the same observer and the average of the results was utilised in the study.

Each subject was identified as having either a type 1, type 2 or intermediate lunate (Moojen et al., 2002; Nakamura et al., 1997; Viegas, 1990; Viegas et al., 1993; Viegas et al., 1990). The measurements of the scaphoid were performed as first described by Craigen and Stanley (Craigen and Stanley, 1995) and replicated by Garcia-Elias et al (Garcia-Elias et al., 1995).

The scaphoid length was measured in ulnar deviation (R1) and radial deviation (R2). Scaphoid translation across the radius was measured in radial (R3) and ulnar deviation (R4) (Figure 2.13).

From these initial data measurements a number of calculations were made. Calculations as reported by Craigen and Stanley (Craigen and Stanley, 1995) were performed. These included the CR index and the translation ratio. The CR index was defined as R2/R1. A perfect “row” wrist would have a CR index = 1, while a “column” wrist would have a CR index of approximately 0.5. The translation ratio is defined as ([R3-R4]/R1).

Calculations as reported by Garcia-Elias et al (Garcia-Elias et al., 1995) were performed. These included scaphoid flexion index (SFI), the scaphoid inclination index (SII) and the scaphoid kinematic index (SKI). The SFI represents the amount of flexion-extension of the scaphoid and is the change in length of the scaphoid expressed as a percentage of the total length of the scaphoid in ulnar inclination. The SII represents the amount of radio-ulnar deviation of the scaphoid. The SKI is the ratio between the two (SKI = SFI/SII). This investigation stated that a wrist with an SKI>1 had more scaphoid flexion-extension than radio-ulnar inclination and vice versa if the SKI was smaller than 1.

The relationships between lunate type and CR index, translation ratio, SFI, SII and SKI were analysed using Pearson’s correlation coefficients.

3.2.4 Main finds of the published research

There was a statistically significant difference between the type 1 and type 2 lunates for all the radiographic indices measured.

The CR index demonstrated that the scaphoid associated with the type 2 lunate had a significantly greater degree of flexion during radial deviation. The translation ratio demonstrated that the scaphoid associated with type 1 lunate had a significantly greater degree of translation. The SFI demonstrated that the scaphoid associated with type 1 lunate had significantly less flexion-extension compared to the type 2 lunate wrist.

The SII demonstrated that the scaphoid associated with a type 1 lunate translates to a significantly greater degree than a scaphoid associated with a type 2 lunate (Figure 3.1).

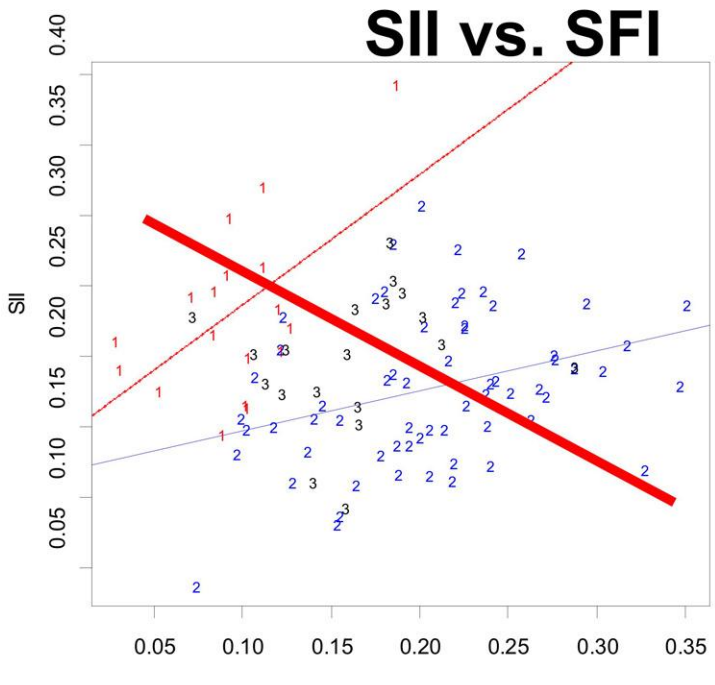

Lunate type	Correlation	Regression equation	R^2
I	0.55 (P=0.018)	SII = 0.144 + 0.927 SFI	25.9%
II	0.33 (P=0.008)	SII = 0.119 + 0.284 SFI	9.7%

Figure 3.1 - Demonstrates the results obtained from the author's patient population. It is interesting to compare the author's results with those published by Garcia Elias (Figure 2.13) SII (scaphoid inclination index), SFI (scaphoid flexion index) The results for each individual are marked with a number to represent the lunate type, i.e. 1, 2 or 3 (intermediate). Red line is the correlation of the total group. The thin red line is for the correlation of the type 1 lunate wrists and thin black line is for the correlation of the type 2 lunate wrists.

The SKI was low for the scaphoid associated with a type 1 lunate. This demonstrates that a type 1 lunate has a strong association with a row type of wrist as initially described by Garcia-Elias et al (Garcia-Elias et al., 1995). In comparison, the scaphoid associated with a type 2 lunate had a high SKI, which demonstrates that it behaves as a column wrist.

3.3 An anatomic study of the triquetro-hamate joint

3.3.1 Research aims

The study on the triquetro-hamate joint presented in the thesis aimed to determine the morphology of this joint. To postulate the kinematic consequences of the morphological factors identified.

3.3.2 Research objectives

To observe the anatomical characteristics of the dry and wet specimens of the triquetrum and hamate bones.

To assess whether there are different types of triquetrum and hamate bones and to determine what the characteristic features of each type are.

To assess whether there are different types of triquetro-hamate joint and to determine what the characteristic features of each type are.

To determine if the type of lunate (Viegas, 1990) is a correlated to the types of hamate, triquetrum or triquetro-hamate joint.

3.3.3 Principles of study methodology

Dry osseous specimens of the wrist were examined.

Embalmed cadaveric wrist specimens were exposed via a dorsal arthrotomy and inspected with loupe magnification.

The shape of the joint surfaces was investigated, with particular reference to the various shapes of the hamate and triquetrum and how they articulated with each other.

The type of lunate as reported by Viegas was assessed (Viegas, 1990).

3.3.4 Main findings of the published research

Two distinct types of hamate were identified that were designated type 1 and 2 (Figure 3.2).

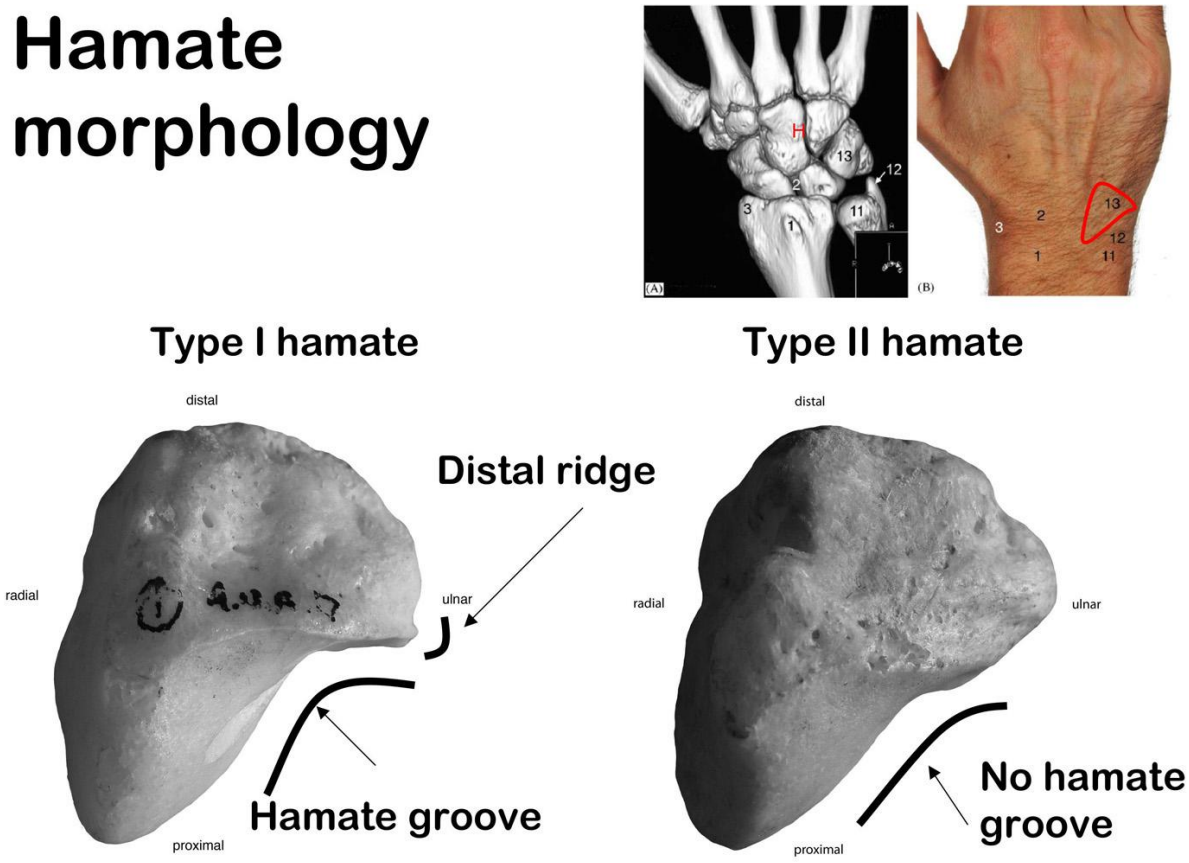

Figure 3.2 – Hamate, dorsal view (A) a right type I hamate and (B) a type 2 hamate. The type 1 hamate with a deep hamate groove and a distinct distal ridge. The type 2 hamate has a shallow hamate groove and no distal ridge.

Two distinct types of triquetrum that were designated type A and type B (Figure 3.3). There was also an intermediate group.

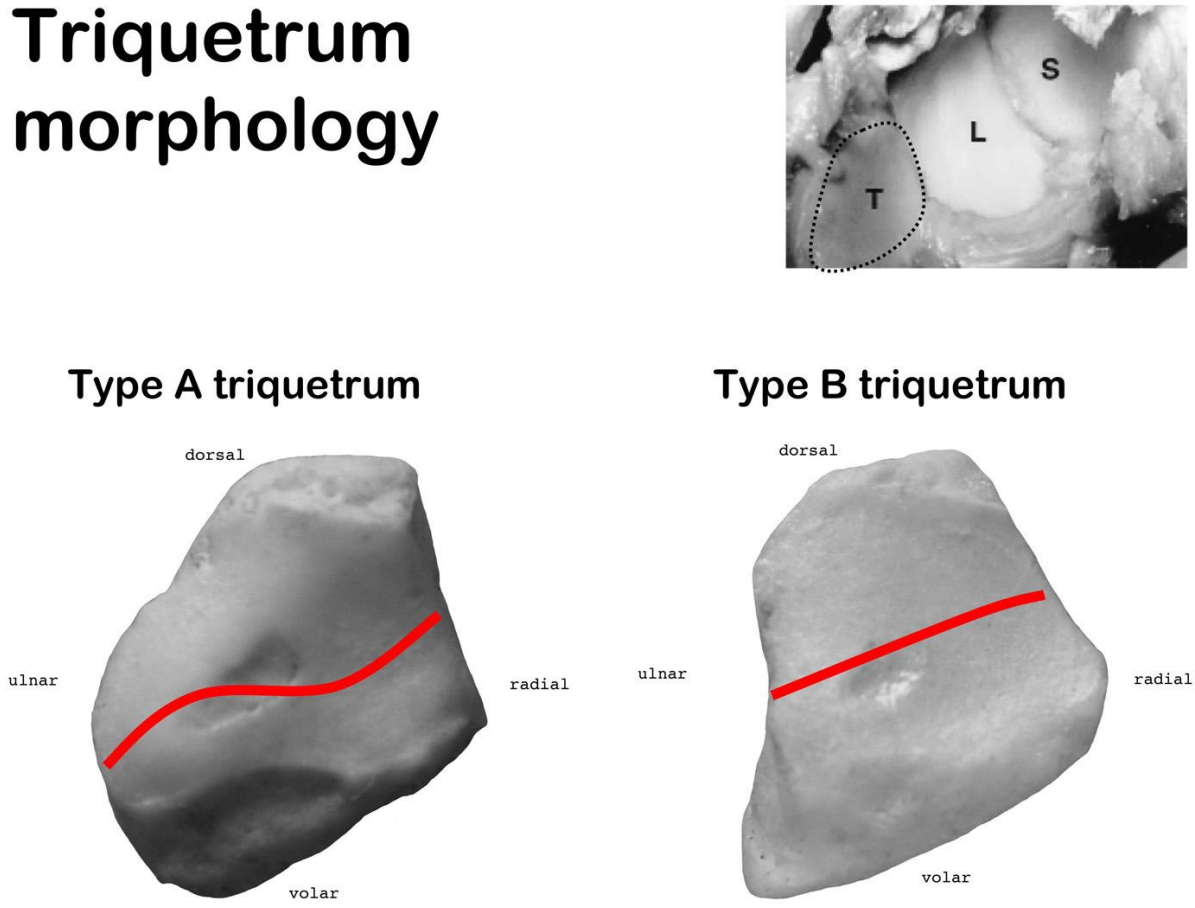

Figure 3.3 – Triquetrum, mid-carpal view (A) right type A triquetrum and (B) a type B triquetrum. The type A triquetrum has a helicoidal shape. The type B triquetrum has a flat dish shape.

The corresponding articulation patterns of these joint surfaces showed a strong trend for a type A triquetrum to articulate with a type 1 hamate and for a type B triquetrum to articulate with a type 2 hamate.

These two distinct types of triquetro-hamate articulations were designated type 1 (TqH-1) and 2 (TqH-2) triquetro-hamate joint (Figure 3.4). No association was identified between lunate type and hamate type.

The TqH-1 joint is double-faceted and helicoidal in configuration. It is a surface designed to transmit a rotational torque. With the TqH-2 joint the hamate and triquetrum surfaces are flatter and possess complementary concave and convex surfaces that are dish shape.

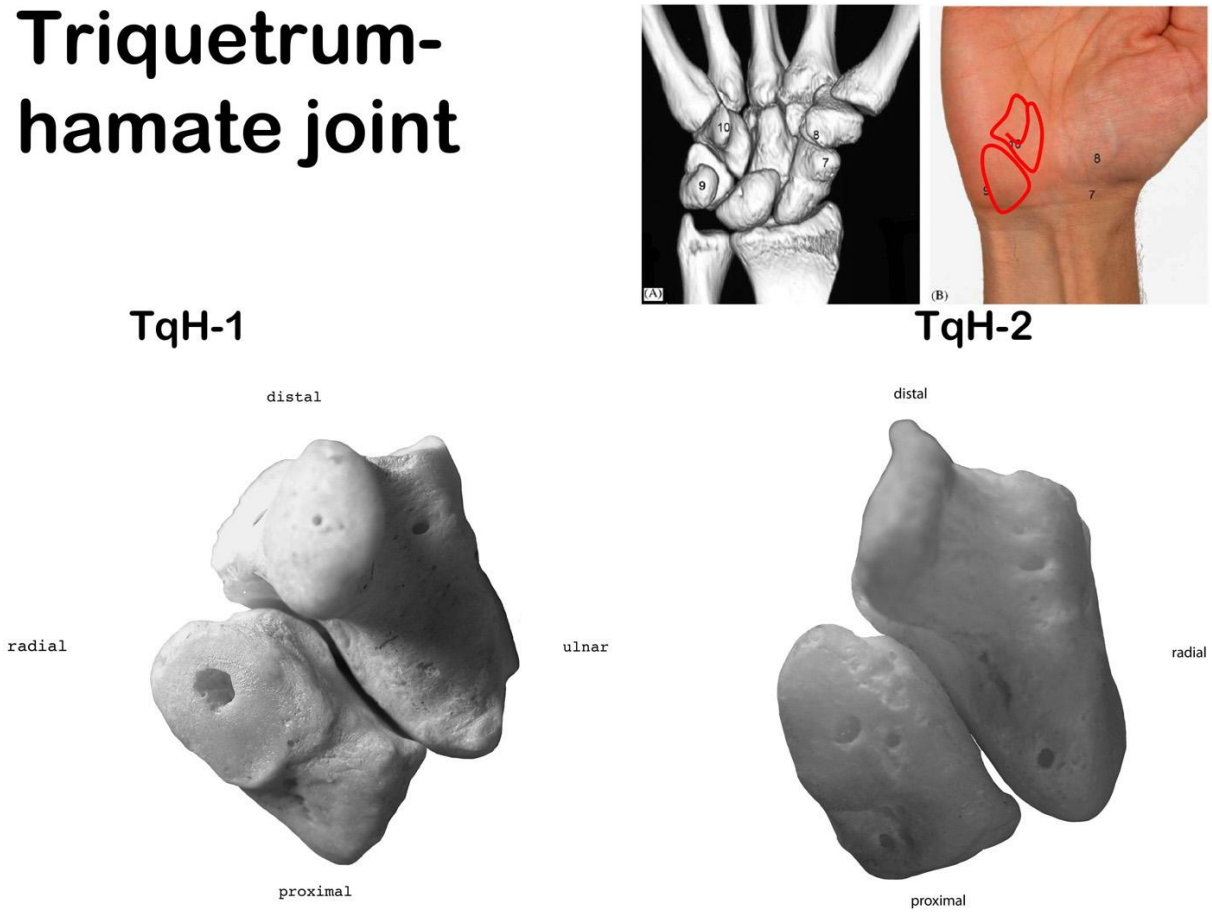

Figure 3.4 – Triquetro-hamate joint, volar view (A) Type TqH-1 joint. Note the biconcave articulation between a type A triquetrum and type I hamate. (B) Type TqH-2 joint. Note the dish shaped articulation between a type B triquetrum and type II hamate.

Chapter 4 - RESEARCH UNDERTAKEN - IMAGING

4.1 Introduction

This section provides a review of the research undertaken on the imaging of the wrist. It includes four papers. The first three papers are on longitudinal computed tomography of the scaphoid and include development of a standardised technique, assessment of the humpback deformity and the clinical utilisation of CT scanning of the scaphoid. The final paper is on the role of fluoroscopy in surgery for the upper limb.

4.2 Longitudinal computed tomography of the scaphoid

4.2.1 Research aims

To develop a standardised technique for imaging of the scaphoid that is clinical useful

4.2.2 Research objectives

1. To review patient tolerance of the technique.
2. To assess the image quality for artefact from the radius.
3. To assess the images to confirm that they are in the longitudinal plane.
4. To review clinical images of cases where the technique has utilised for its clinical utility.

4.2.3 Principles of study methodology

Development of technique
Various techniques of performing CT scanning were trialled

4.2.4 Main findings of the published research

Initially patients had CT scans performed in ulnar deviation (as is often performed with plain radiographs). However patients did not tolerate this position and motion artefact was often observed.

The authors identified that patients were more comfortable when imaging the scaphoid with the wrist in radial deviation and that an immobilisation device was not required (Figure 4.1).

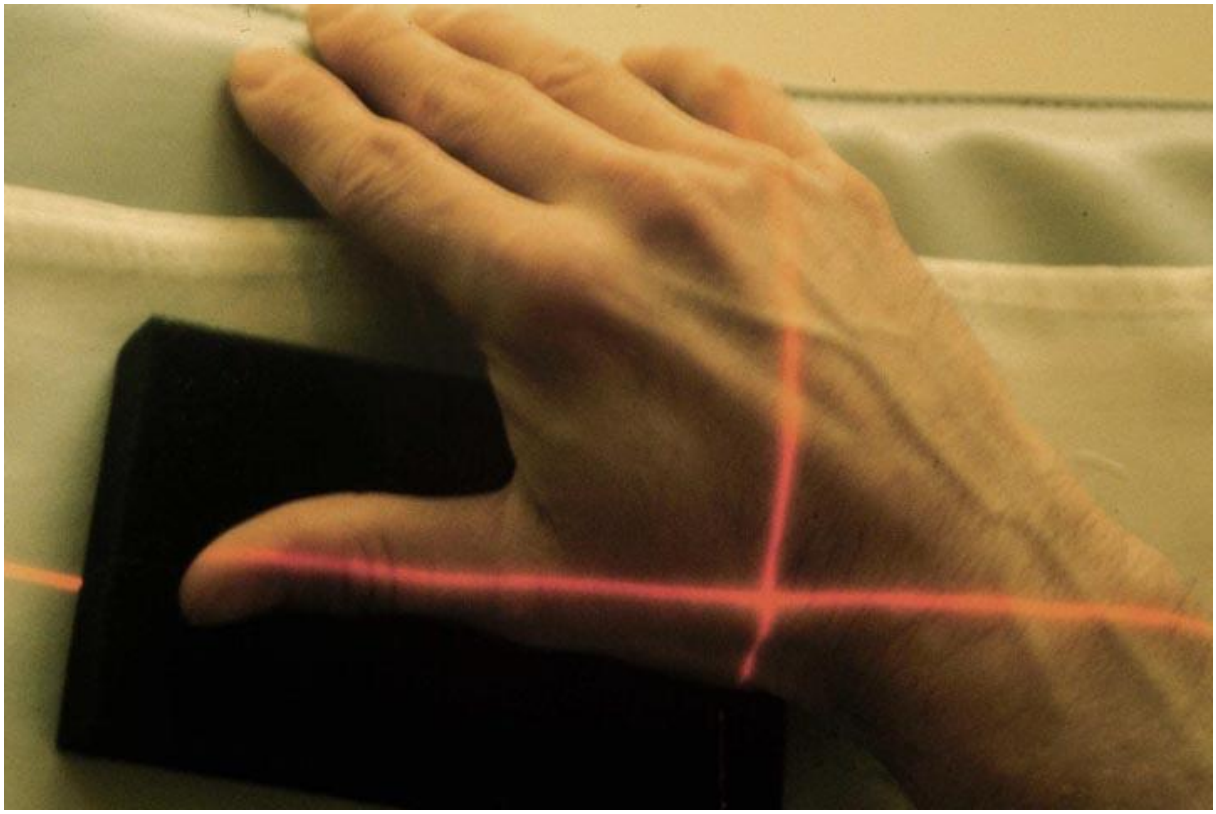

Figure 4.1 – Longitudinal CT scan of the scaphoid with the wrist held in radial deviation. From - Bain et al., 1995.

The initial scout images were along the first web space, but this often led to an incorrect scanning plane and the need to reposition the wrist.

The authors identified that if the scout image was orientated along the line of the first metacarpal that this approximated the longitudinal axis of the scaphoid. The “target sign” confirmed that the scanning plane was along the longitudinal axis of the scaphoid (Figure 4.2).

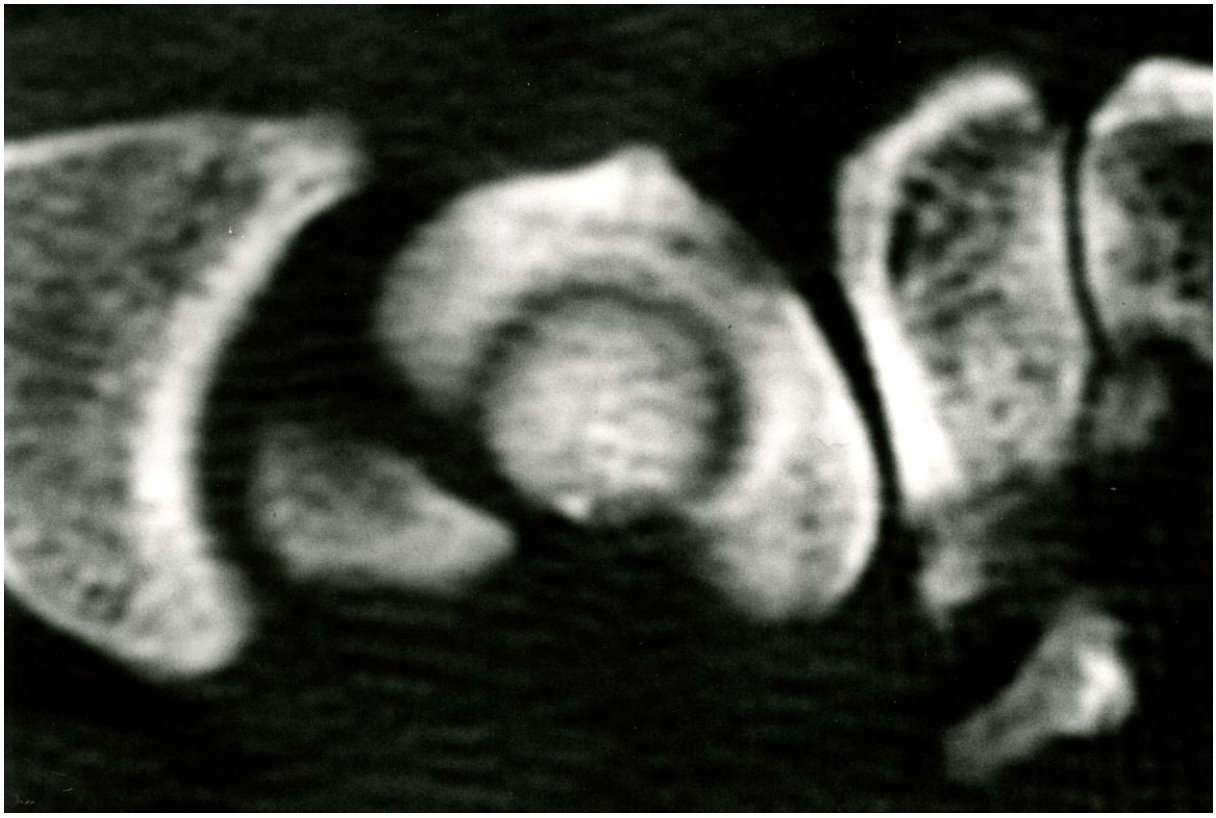

Figure 4.2 – The target sign. Longitudinal CT scan of the left wrist. The head of the capitate is between the proximal and distal poles of the scaphoid. It is objective evidence that the scan is along the longitudinal axis of the scaphoid. From - Bain et al., 1995.

The images obtained demonstrated the detail of anatomy such that an understanding of the clinically relevant concerns of the scaphoid could be obtained. This included assessment of fracture location, deformity and union.

Placing the wrist in radial deviation rotated the image plane away from the shaft of the radius to reduce artifact.

In radial deviation the humpback deformity was accentuated (Figure 4.3).

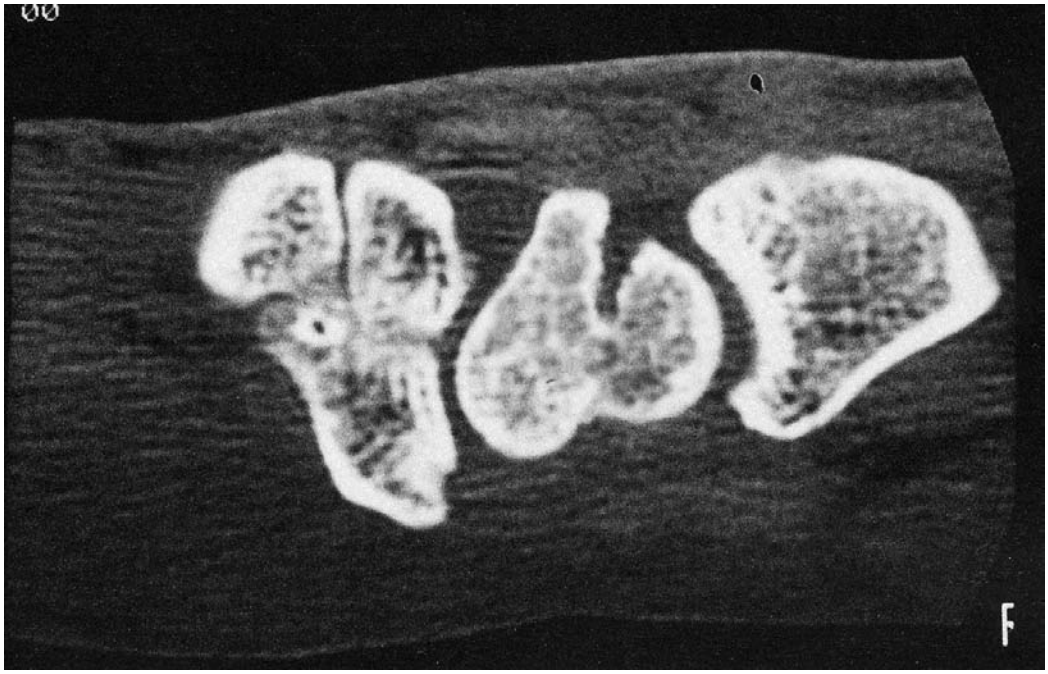

Figure 4.3 - Humpback deformity. Longitudinal CT scan of the right wrist. The proximal pole of the scaphoid is extended and the distal pole flexed. It produces carpal shortening. From - Bain, 1999.

As a consequence of the technique being clinically valuable, a protocol for utilising the technique was established (Appendix 4.1). This became the standard method for longitudinal computed scanning of the scaphoid for the remainder of the thesis.

With the use of the target sign, a standardised method for performing longitudinal CT scans is obtained (Figure 4.1).

4.3 Measurement of the scaphoid humpback deformity using longitudinal computed tomography

4.3.1 Research aims

The aim is to better understand the deformities of the scaphoid.

4.3.2 Research objectives

1. To develop new methods of assessment of scaphoid deformity.
2. To compare the intra-observer and inter-observer variability of measurement of scaphoid fractures using published and developed techniques.
3. To measure normal scaphoid without deformity to document their indices.

4.3.3 Principles of study methodology

A series of longitudinal CT scans of the scaphoid were chosen at random from a group of scans performed over a one year period. This series included a spectrum of scaphoid pathologies. The scans were performed using the protocol technique developed in the previous paper (Appendix 4.1). Scans were excluded if the scanning plane did not correspond to the longitudinal axis of the scaphoid.

Each scan was assessed by three observers. Acetate sheets were placed over the scans so that any lines drawn by one observer could not influence another.

Each observer measured the humpback deformity using all three techniques. The observers had no other clinical or radiologic information and were not aware of the other observers' measurements. Each observer repeated the measurements after an interval of at least one week.

Measurement Techniques

A modification of the lateral intrascaphoid angle described by Amadio et al was measured. The dorsal scaphoid angle (Figure 4.4) and the height-to-length ratio (Figure 4.5) were calculated. The measurements were statistically analysed and intra-observer and inter-observer reliability was assessed by intraclass correlation coefficients (ICCs) (Shrout and Fleiss, 1979).

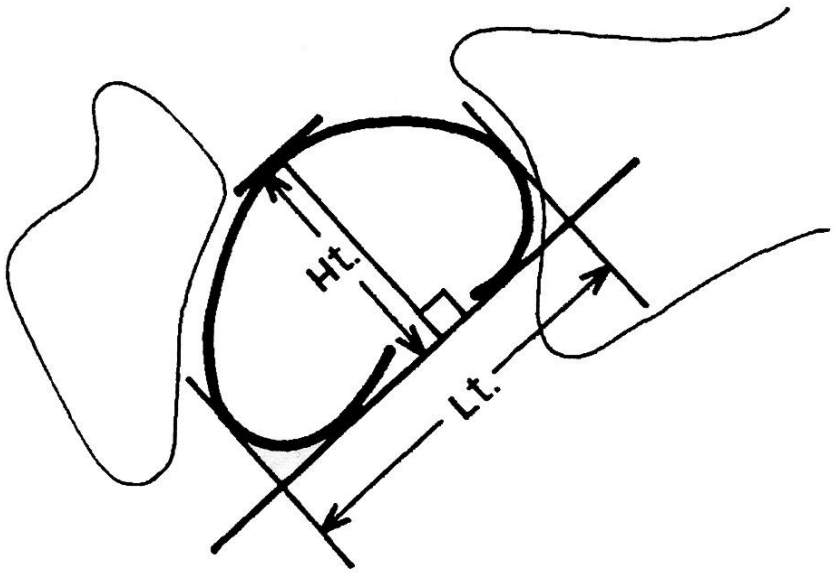

Figure 4.4 – Height-to-length ratio. A baseline is drawn along the volar aspect of the scaphoid. The length of the scaphoid along the baseline is measured, as is the height of the scaphoid perpendicular to the baseline. The height-to-length ratio is recorded as a percentage. From - Bain et al., 1998.

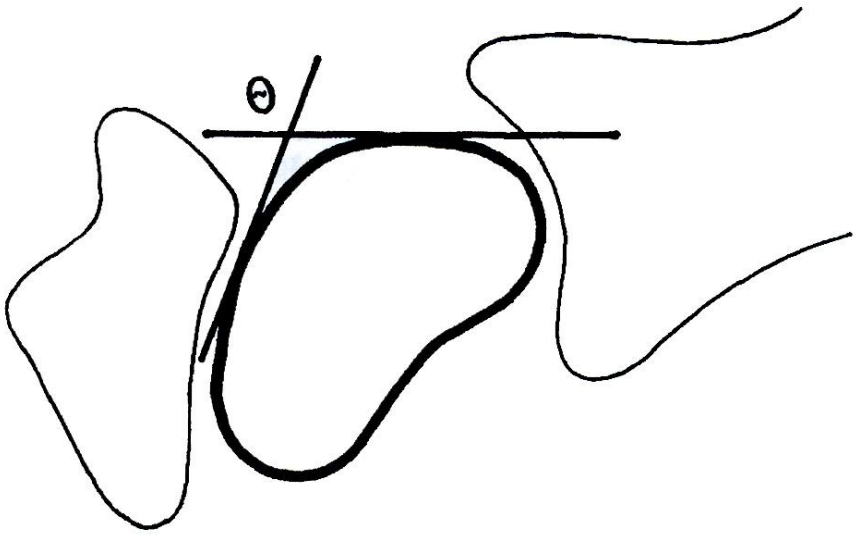

Figure 4.5 – Dorsal cortical angle. A line is drawn along the dorsal cortex of the proximal and distal halves of the scaphoid and the angle between these lines is measured. From - Bain et al., 1998.

4.3.4 Main findings of the published research

The intraobserver reliability of the intrascaphoid angle was poor; the dorsal cortical angle was moderate to excellent and the height-to-length ratio was excellent. The inter-observer reliability of the intrascaphoid angle was poor to moderate, the dorsal cortical angle was moderate to excellent and the height-to-length ratio was moderate to excellent. For all three observers the intra-observer and inter-observer reliability was the best for the height-to-length ratio and worst for the intrascaphoid angle. The height-to-length ratio is the most reliable method of assessing the humpback deformity.

The values for the normal scaphoid that did not have a deformity were also reported for the different measurement methods.

4.4 Clinical utilisation of computed tomography of the scaphoid

4.4.1 Research aims

The aim of this study was to provide an overview of the role of computed tomography for the management of scaphoid fractures.

4.4.2 Research objectives

1. To determine the factors that lead to a difference in inter-observer variability when assessing scaphoid fracture union.
2. To determine the cases in which computed tomography should be considered in clinical practise.
3. To develop a pre-operative method of assessing correction of the humpback deformity.

4.4.3 Principles of study methodology

A series of CT scans of the scaphoid were assessed for scaphoid deformity and fracture union.

4.4.4 Main findings of the published research

In clinical cases in which only a few trabeculi appeared to cross the fracture there was discrepancy between assessors. Partial volume averaging (Figure 4.6) explains some of the cases in which differences of opinion occurred in assessment of union of a scaphoid fracture. This was based on unpublished work where observers were asked to identify fracture union and percentage of fracture union. The cases in which a discrepancy occurred were those in which some observers thought the fracture was united and other observers thought it was not united. Those cases usually had less than 20% union. The operative findings demonstrated a fracture non union in these cases.

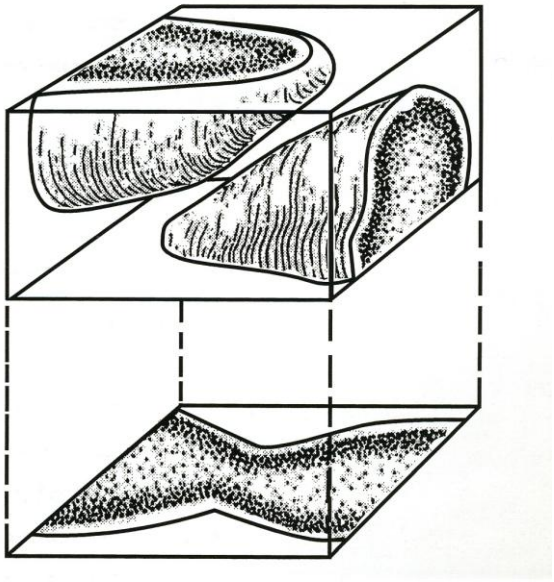

Figure 4.6 – Partial volume averaging. A three-dimension "slice" of tissue is computed to produce a two-dimensional image. A non union which passes obliquely through a "slice" may appear united as there is some bone within the slice which will appear on the two-dimensional image as an incomplete union. From - Bain, 1999.

The pre-operative assessment of scaphoid fracture deformity and planning to correct the deformity with a templating technique was presented **(**Figure 4.7). This method ensures that the correct surgical approach is used, the correct graft size is known pre-operatively and that the correct fixation method is used.

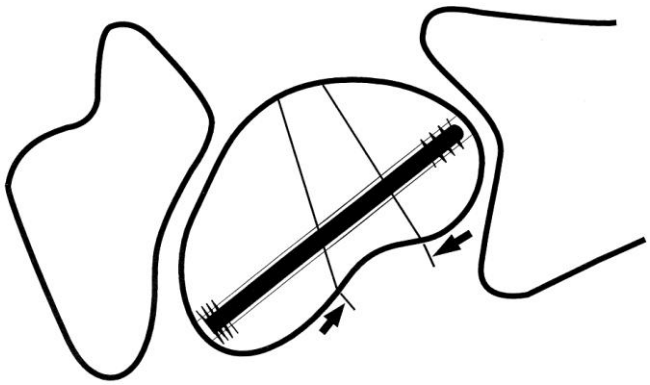

Figure 4.7 – Diagram demonstrating a longitudinal CT scan representation of right wrist. Pre-operative CT scan "template". The trapezoidal bone graft and screw in situ is useful to determine the need for a structural bone graft, the preferred fixation screw, and to assess whether it should be inserted via a volar or dorsal approach. From - Bain, 1999.

4.5 Operative fluoroscopy in hand and upper limb surgery

4.5.1 Research aims

The aim is to assess the clinical value of fluoroscopy to the surgeon for management of disorders of the upper limb.

4.5.2 Research objectives

1. To document the cases in which the fluoroscopic unit was utilised.
2. To assess the types of cases in which the device is of value to the operating surgeon.
3. To assess the limitations of the fluoroscopy units in management of clinical cases.
4. To review the legislative requirements of the device for the clinic.

4.5.3 Principles of study methodology

Patients on whom the device was used were recorded prospectively on an operative database, which was subsequently reviewed.

The spectrum of clinical cases was reviewed and categorised.

4.5.4 Main findings of the published research

The portable fluoroscopy is a useful device for management of wrist and upper limb traumatic and degenerative disorders.

The use of fluoroscopy with arthroscopy was an important addition to the surgical management of disorders such as distal radius fractures. It was valuable to assess the position of fixation, but also to assess the stability of the fracture fixation. If instability of the fixation was identified then further fixation would be added. The paper highlighted the importance of fluoroscopy when performing provocation tests such as for mid-carpal instability. Prior to this time it was common for radiologists to perform fluoroscopic assessment of the wrist at the radiology department. However, the best option is for the surgeon to perform the provocation tests on the patient under fluoroscopy. The low dose portable unit is ideal for such tests.

The use of diagnostic injection techniques into the localised joint spaces such as the thumb CMC joint and DRUJ are important. The surgeon can be sure that the injection is in the joint

and he has the opportunity to observe the effect of the local anaesthetic.

The limited working distance within the C arm, with large bone procedures, was documented, e.g. insertion of intra-medullary nails for humeral shaft fractures.

The legal requirements were reviewed and documented.